

**Self-Powered Flexible Humidity Sensor Based on
Moisture-induced Electric Generation**

Wong Ke Xin

UNIVERSITI TUNKU ABDUL RAHMAN

**Self-Powered Flexible Humidity Sensor Based on
Moisture-induced Electric Generation**

Wong Ke Xin

**A project report submitted in partial fulfilment of the
requirements for the award of Bachelor of Science
(Honours) Physics**

**Lee Kong Chian Faculty of Engineering and Science
Universiti Tunku Abdul Rahman**

May 2025

DECLARATION

I hereby declare that this project report is based on my original work except for citations and quotations which have been duly acknowledged. I also declare that it has not been previously and concurrently submitted for any other degree or award at UTAR or other institutions.

Name : Wong Ke Xin

ID No. : 2102608

Date : 12/05/2025

COPYRIGHT STATEMENT

© 2025, WONG KE XIN. All right reserved.

This final year project report is submitted in partial fulfilment of the requirements for the degree of Bachelor of Science (Honours) Physics at Universiti Tunku Abdul Rahman (UTAR). This final year project report represents the work of the author, except where due acknowledgement has been made in the text. No part of this final year project report may be reproduced, stored, or transmitted in any form or by any means, whether electronic, mechanical, photocopying, recording, or otherwise, without the prior written permission of the author or UTAR, in accordance with UTAR's Intellectual Property Policy.

ACKNOWLEDGEMENTS

I would like to express my deepest gratitude to Dr. Tan Chun Hui, my research supervisor, for his invaluable advice, continuous guidance, and immense patience throughout the development of this final year project. His expertise and encouragement have been vital to the successful completion of this research.

My heartfelt thanks also go to Mr. Vinod K Ganesan, a PhD student under Dr. Tan Chun Hui who has consistently guided me with technical insights, constructive feedback, and motivational support during every stage of the project.

I would also like to thank Dr. Lee Soon Poh for providing helpful advice and suggestions, which have been beneficial to my understanding and refinement of the project.

I am grateful to the Lee Kong Chian Faculty of Engineering and Science, University Tunku Abdul Rahman (UTAR), and all faculty and departmental members of the Department of Electrical and Electronic Engineering for creating a supportive and pleasant research environment throughout my studies.

Lastly, special thanks to my dearest friends, Gan Ming You and Tan Kang Yi, for their unwavering support, encouragement, and friendship during the most challenging moments of this journey. Their presence and positivity have been instrumental to the completion of this project.

ABSTRACT

Conventional humidity sensors often suffer from limited flexibility and reliance on external power sources, hindering their integration into low-cost, sustainable, and portable systems. This study presents the development of a flexible self-powered humidity sensor based on moisture-induced electricity generation (MEG), utilizing laser-induced graphene (LIG) fabricated on lignin-coated paper. A commercially available 5 V violet laser engraver (405 nm) was employed to induce graphitization through a simple, single-step scribing process. Fabrication was optimized by varying the paper's tilt angle (0° to 20°) to enhance voltage output and stability. Surface morphology and elemental composition were analyzed using SEM, EDX, and XRD. Under 80% relative humidity, the sample fabricated at 20° tilt angle generated the highest average voltage (~ 6.5 mV) but showed unstable performance. In contrast, the sample prepared at 15° produced a slightly lower voltage (~ 4.2 mV) with significantly greater stability, identifying it as the optimal configuration. These findings demonstrate the potential of LIG-based MEG as a cost-effective, battery-free humidity sensing solution and offer insights into scalable fabrication strategies for flexible electronics.

Keywords: humidity sensor; self-powered sensor; laser-induced graphene; moisture-induced electricity generation; flexible electronics

Subject Area: TA165 Engineering instruments, meters, etc. Industrial instrumentation

TABLE OF CONTENTS

DECLARATION	i
ACKNOWLEDGEMENTS	iii
ABSTRACT	iv
TABLE OF CONTENTS	v
LIST OF TABLES	vii
LIST OF FIGURES	viii

CHAPTER

1	INTRODUCTION	1
	1.1 General Introduction	1
	1.2 Importance of the Study	2
	1.3 Problem Statement	2
	1.4 Objectives	3
	1.5 Scope and Limitation of the Study	3
	1.6 Contribution of the Study	3
	1.7 Outline of the Report	4
2	LITERATURE REVIEW	5
	2.1 Introduction to Humidity Sensor	5
	2.2 Self-Powered Sensors	23
	2.3 Moisture-Induced Electricity Generation	30
	2.4 Laser-Induced Graphene	36
	2.5 Summary	41
3	METHODOLOGY AND WORK PLAN	43
	3.1 Introduction	43
	3.2 Equipment and Materials	44
	3.3 Methodology	45
	3.4 Performance Evaluation under Controlled Humidity Conditions	47
	3.5 Summary	48

4	RESULTS AND DISCUSSION	50
4.1	Introduction	50
4.2	Morphological and Structural Analysis	50
4.3	Influence of Laser Tilting Angle on Voltage Output and Stability	53
4.4	Voltage Response of the Optimized Sample to Varying Humidity Levels	56
4.5	Summary	58
5	CONCLUSIONS AND RECOMMENDATIONS	60
5.1	Conclusions	60
5.2	Recommendations for future work	61
	REFERENCES	62

LIST OF TABLES

Table 2.1.1:	Relevant Properties of Humidity Sensors.	7
Table 2.1.2:	Overview of Different Types of Humidity Sensors.	19
Table 2.4.3:	Key Laser Parameters Affecting LIG Formation	40

LIST OF FIGURES

Figure 2.1.2 (a):	Capacitive humidity sensor with interdigitated electrodes.	8
Figure 2.1.2 (b):	Relationship of capacitive change to humidity.	9
Figure 2.1.2 (c):	Resistive humidity sensor with hygroscopic sensing material.	10
Figure 2.1.2 (d):	Relationship of resistive change to humidity.	11
Figure 2.1.2 (e):	Optical humidity sensor detects changes via cobalt chloride-gelatin film, with unmodified fiber as reference.	13
Figure 2.1.2 (f):	Thermal Conductivity Humidity Sensor.	15
Figure 2.1.2 (g):	Chilled mirror hygrometers.	16
Figure 2.1.2 (h):	Aluminum oxide moisture sensors.	18
Figure 2.2.3 (a):	Flexible solar-based wearable energy harvester.	24
Figure 2.2.3 (b):	(left) Measured output of flexible PV panel. (right) Flexible PV panel voltage with MPPT control under a lighting intensity of 320 lux.	25
Figure 2.2.3 (c):	Schematic sketch of direct (a) and indirect (b) piezoelectric effects.	25
Figure 2.2.3 (d):	(a) Application of self-powered respiratory sensor in face-mask. (b) Output voltage upon slow inhale/exhale conditions of five different candidates. (c) Output voltage upon slow and fast inhale/exhale conditions of the same candidates. (d) Stable output voltage response over a period of time. (e) Charging of 0.1 μ F capacitor using the output voltage upon continuous inhale/exhale.	26
Figure 2.2.3 (e):	(left) Output voltage during walking. (right) Voltage output of human pulse test.	26
Figure 2.2.3 (f):	Schematic sketch of thermoelectric generators.	27
Figure 2.2.3 (g):	Pulse oximeter powered by watch-style thermoelectric generator.	27
Figure 2.2.3 (h):	MEMS vibrational energy harvester.	28

Figure 2.3:	Schematic mechanism of MEG.	30
Figure 2.3.1 (a):	MEG using gradient material.	31
Figure 2.3.1 (b):	(a) Schematic representation of the electric double layer forming at the solution–solid interface. (b) Schematic depiction of the classical electrokinetic effect within a nanochannel.	32
Figure 2.3.1 (c):	Charge build-up and discharge of electrodes in a capacitor.	33
Figure 3.3.1:	Preparation of coating solution.	45
Figure 3.3.2:	Coating filter paper.	46
Figure 3.3.3:	Schematic of MEG fabrication. Laser scribing with a gradual defocusing method.	46
Figure 3.4:	Voltage performance testing under set humidity conditions.	47
Figure 4.2.1:	SEM test of the LIG sample.	51
Figure 4.2.2:	EDX spectrum of the LIG sample.	52
Figure 4.2.3:	XRD spectrum of the LIG sample.	53
Figure 4.3 (a):	Average voltage output of LIG samples at varying tilt angles under 80% RH.	53
Figure 4.3 (b):	Voltage output of LIG samples at varying tilt angles under 80% RH over time.	54
Figure 4.4:	Voltage output under different relative humidity levels.	56

CHAPTER 1

INTRODUCTION

1.1 General Introduction

In recent years, advancements in low-power and flexible electronics have fueled growing interest in energy-autonomous sensor systems, particularly for applications in environmental monitoring, wearable technology, and healthcare. Among these, humidity sensors play a vital role in detecting atmospheric moisture, which is crucial in areas such as agriculture, indoor air quality control, respiratory diagnostics, and smart packaging. However, traditional humidity sensors rely heavily on external power sources, limiting their long-term deployment and integration into portable or flexible systems.

To overcome this limitation, the concept of self-powered sensors has gained significant attention. Moisture-enabled electricity generation (MEG), also referred to as hygroelectricity, has emerged as a promising mechanism for harvesting ambient moisture to power sensing devices. Materials such as graphene oxide (GO) and laser-induced graphene (LIG) have demonstrated the ability to generate electricity through interactions with water molecules, primarily via ion dissociation and transport within gradient structures. Paper substrates – valued for their flexibility, biodegradability, and low cost – have become attractive platforms for developing such sensors.

This project focuses on the development of a self-powered, flexible humidity sensor based on MEG, utilizing a lignin-coated paper substrate. Laser scribing is employed to induce structural and functional asymmetry in the LIG layer, enhancing both energy generation and sensing performance.

1.2 Importance of the Study

The development of sustainable, low-cost, and energy-independent sensors is essential to realizing the vision of next-generation smart devices. Self-powered sensors eliminate the need for frequent battery replacement or external power sources, thereby reducing environmental impact and enabling continuous operation in remote or wearable applications. By integrating moisture-induced electricity generation with flexible paper-based materials, this study aligns with current trends in green electronics and Internet of Things (IoT) applications.

Furthermore, understanding how fabrication techniques – such as laser processing – influence the ion transport and voltage generation mechanisms offers valuable insights for optimizing sensor design. This study not only presents a novel approach to humidity sensing but also contributes to the broader advancement of energy harvesting technologies.

1.3 Problem Statement

Conventional humidity sensors are constrained by their reliance on external power sources, rigid substrates, and complex manufacturing processes. These limitations hinder their integration into flexible, portable, and disposable systems. Although some progress has been made using nanomaterials for energy harvesting, the mechanisms underlying moisture-induced electricity generation (MEG) and their effective integration into functional sensor systems remain insufficiently explored. Additionally, the optimization of fabrication parameters – such as laser-induced structural modulation – and their role in enhancing MEG performance are not yet fully understood. There is a need to investigate and characterize self-powered sensing platforms that are both efficient and compatible with flexible, low-cost materials.

1.4 Objectives

1. To develop and characterize a self-powered, flexible humidity sensor based on moisture-enabled electricity generation (MEG) on paper substrates.
2. To investigate the electricity generation mechanism influenced by ion concentration gradients induced through laser processing.
3. To evaluate the performance, stability, and reliability of the sensor under varying humidity conditions.

1.5 Scope and Limitation of the Study

This study focuses on the fabrication of LIG-based humidity sensors using lignin-coated paper as a flexible substrate. Laser processing parameters, particularly tilt angle and defocus, are varied to induce functional gradients and porous structures that enhance MEG. The research includes material characterization using SEM, EDX, and XRD, along with performance evaluation under controlled humidity environments.

However, the scope is limited to evaluating voltage output under ambient laboratory conditions. The sensor is not integrated into a complete electronic system, nor is long-term field testing conducted. Additionally, the study primarily investigates moisture-induced proton transport mechanisms and does not extensively examine multi-ion interactions or the effects of other environmental variables such as temperature or pressure.

1.6 Contribution of the Study

This study contributes to the advancement of self-powered sensor technology by presenting a cost-effective and environmentally friendly method for fabricating humidity sensors on flexible paper substrates using laser-induced graphene (LIG). It provides experimental validation of MEG in LIG-based devices and offers new insights into the relationship between structural gradients, surface properties, and ion transport efficiency. The findings deliver practical study for optimizing laser defocus to enhance energy harvesting and sensing performance, with potential applications extending to other types of sensors and bioelectric devices.

1.7 Outline of the Report

This report is structured as follows:

- **Chapter 1** introduces the background, motivation, problem statement, objectives, and contributions of the study.
- **Chapter 2** presents a literature review covering recent advances in humidity sensors, self-powered mechanisms, moisture-induced electricity generation (MEG), and LIG fabrication techniques.
- **Chapter 3** describes the experimental methodology, including materials, fabrication procedures, characterization methods, and testing setups.
- **Chapter 4** discusses the experimental results, analyses the voltage output behaviour under fixed and varying humidity, and interprets the MEG mechanism based on the fabricated structures.
- **Chapter 5** concludes the study by summarizing the key findings, highlighting the significance of the work, and suggesting future directions for improving and expanding the sensor's applications.

CHAPTER 2

LITERATURE REVIEW

2.1 Introduction to Humidity Sensor

A sensor is a device that detects physical or environmental changes and converts them into signals that can be measured, processed, and interpreted by humans or machines. These signals can be electrical, optical, or mechanical and may represent a wide range of variables, such as temperature, pressure, motion, light intensity, sound, humidity, or chemical composition. It acts as an interface between the physical world and electronic systems, enabling the measurement of various physical phenomena.

Humidity refers to the amount of water vapor present in the air or any gaseous environment. It plays an important role in weather forecasting, human comfort, material properties, and the performance of electronic devices. As a result, measuring humidity is essential in fields such as meteorology, agriculture, healthcare, and industrial production.

A humidity sensor is a device designed to measure the moisture level in the air. It detects the amount of water vapor present in the environment and converts this data into measurable signals. According to National Weather Service (2015), humidity measurements are commonly expressed in terms of:

- i. **Absolute Humidity (AH):** The actual amount of water vapor in the air, independent of temperature. This value represents the mass of water vapor per unit volume of air (g/m^3) and is particularly useful in industrial processes that require precise moisture control or trace moisture detection.
- ii. **Relative Humidity (RH):** The percentage (%) of water vapor present in the air relative to the maximum amount the air could hold at a given temperature. This measure indicates how saturated the air is with moisture. RH is the most commonly used measurement for humidity assessment in both daily life and industrial applications due to its ease

of interpretation and practicality. RH sensors are compact, cost-effective, and easy to integrate into a variety of systems.

- iii. Dew Point Temperature:** The temperature ($^{\circ}\text{C}$ or $^{\circ}\text{F}$) at which air becomes saturated with moisture, causing water vapor to condense into liquid. This temperature is independent of the surrounding temperature and provides an absolute measure of the moisture content in the air. Since it directly correlates with the moisture saturation level, the dew point is often used in combination with absolute humidity for applications requiring high precision.

In short, while absolute humidity is essential for industrial and high-precision applications, relative humidity is more commonly used for everyday monitoring due to its simplicity and ease of use. The dew point, though less frequently used for general monitoring, is crucial in environments where precise moisture control is necessary.

The classification of humidity sensors is primarily based on the measurement technique they use. As mentioned earlier, there are two broad categories: relative humidity sensors and absolute humidity sensors. These categories can be further subdivided into different types of sensors, each utilizing specific principles of operation. The sensor types differ in their accuracy, response time, and suitability for different applications.

2.1.1 Properties of Humidity Sensors

The selection of a humidity sensor depends on factors such as measurement range, accuracy requirements, environmental conditions, and application-specific constraints, all of which influence the sensor's performance. To meet the needs of various applications, a humidity sensor must generally fulfill the following requirements: high sensitivity, high accuracy, a broad operating range for both humidity and temperature, fast response time, excellent repeatability and reproducibility, minimal hysteresis, durability, long lifespan, strong resistance to contaminants, and low fabrication costs. Table 2.1.1 outlines the key properties for sensor functionality.

Table 2.1.1: Relevant Properties of Humidity Sensors.

Parameter	Description
Sensitivity	Ability of the sensor to detect small changes in humidity levels. It is the ratio of change in output signal to change in humidity.
Accuracy	The degree to which the output corresponds to the actual humidity level.
Response Time	The time required for the sensor to stabilize its output after a change in humidity conditions.
Hysteresis	The difference in the sensor's output for the same input, depending on whether the input is increasing or decreasing.
Repeatability	Ability of the sensor to produce the same output when the same input is applied multiple times under the same conditions.
Reproducibility	Ability of the sensor to produce consistent outputs when the same input is applied under different conditions, such as times, locations, or operators.
Drift	The gradual change in the sensor's output over time, even when the input remains constant. Drift is often caused by environmental factors, aging, or material degradation.
Stability	Ability of the sensor to maintain performance over extended periods without significant drift in measurements.

Although most humidity sensors have been developed using various principles to meet diverse application needs, there are still limitations in fully satisfying all requirements simultaneously.

2.1.2 Types of Humidity Sensors

This subsection introduces the most commonly used types of humidity sensors, including capacitive, resistive, optical, thermal conductivity, and hygrometric sensors. The following sections highlight their operating principles, advantages, disadvantages, and recent advancements.

Capacitive Humidity Sensor

Capacitive humidity sensors are among the most commonly used types of humidity sensors, making up approximately 75% of the market due to their widespread applicability and cost-effectiveness (ANDIVI, 2020). These sensors operate by detecting changes in the dielectric constant of a hygroscopic (moisture-absorbing) material, which varies in response to ambient humidity. The core design of a capacitive humidity sensor, as shown in Figure 2.1.2 (a), typically consists of two interdigitated electrodes (IDEs) covering a moisture-sensitive dielectric layer. As the humidity in the environment increases, the dielectric material absorbs water vapor, causing its dielectric constant to change. This variation directly influences the capacitance between electrodes, which is then measured to determine the relative humidity (RH) level.

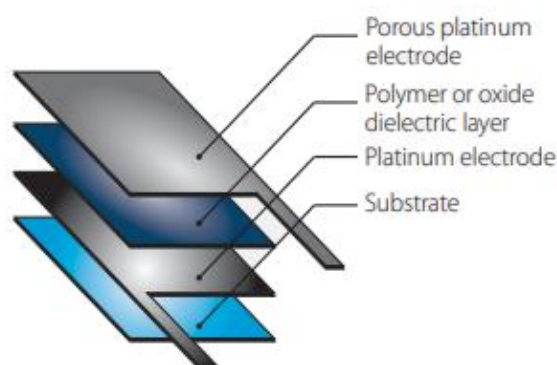


Figure 2.1.2 (a): Capacitive humidity sensor with interdigitated electrodes (ANDIVI, 2020).

The sensing material, typically a thin film deposited between the electrodes, plays a critical role in the sensor's sensitivity and performance. A review by Lee and Lee (2005) briefed that common materials include polyimide films, PMMA (poly(methyl methacrylate)) cross-linked with divinylbenzene (DVB), porous ceramics, and porous silicon, among others.

Each material offers distinct advantages; for example, polyimide films provide high sensitivity but may exhibit hysteresis at high RH levels, while cross-linked PMMA structures help maintain long-term stability by preventing irreversible swelling. Porous materials such as silicon carbide and ceramics are also used for their robustness and stability over time, especially under extreme conditions.

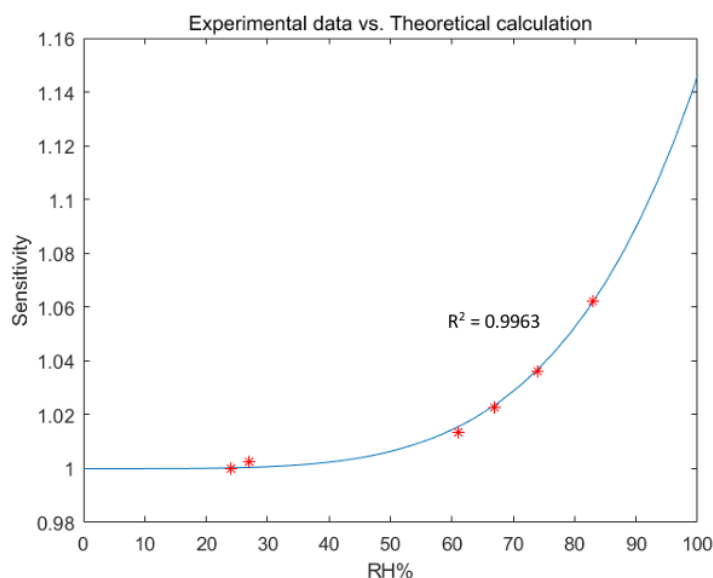


Figure 2.1.2 (b): Relationship of capacitive change to humidity by Yu (2020).

Figure 2.1.2 (b) shows that capacitive humidity sensors exhibit a nonlinear relationship between capacitance and relative humidity, which means that careful calibration is often required to ensure accurate readings across the entire humidity range. Despite this, these sensors are praised for their low power consumption, fast response times, and high output signals. According to Lee and Lee (2005), capacitive sensors are capable of providing reliable measurements even at low humidity levels, with some designs maintaining accuracy down to 0% RH. However, challenges such as hysteresis, improving response time, and temperature dependence can affect sensor performance. Hysteresis, in particular, is a notable drawback because it results from the slower moisture diffusion in the sensing material during the desorption process, which can cause measurement discrepancies.

The advancements in capacitive humidity sensor designs have sought to mitigate these limitations. For instance, integrating micro temperature sensors allows for real-time temperature compensation, which in turn improves the accuracy of humidity readings in varying environmental conditions (Lee and Lee, 2003). Another innovation in the article involves the use of microfabricated cantilevers, where a moisture-sensitive layer is applied to a cantilever structure. As the material absorbs water vapor, the cantilever expands, altering the capacitance and providing a highly sensitive response to humidity changes. Additionally, wireless humidity sensors have been developed, incorporating electroplated copper coils for wireless communication and polyimide film for moisture detection. These sensors offer convenience in applications where physical connections are impractical.

Despite the inherent challenges, such as the potential hysteresis and temperature sensitivity, capacitive humidity sensors remain a popular choice due to their high sensitivity, relatively low fabrication costs, and versatility. Ongoing research and development continue to refine these sensors, addressing their shortcomings while expanding their range of applications, particularly in consumer electronics, HVAC systems, and environmental monitoring.

Resistive Humidity Sensor

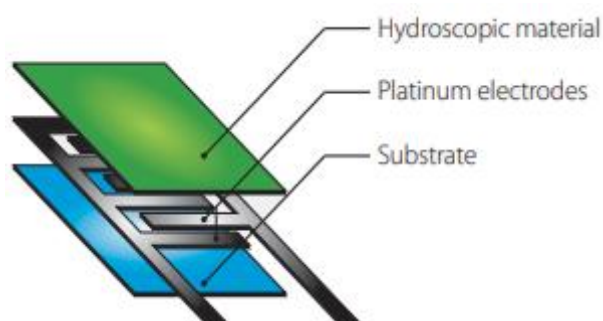


Figure 2.1.2 (c): Resistive humidity sensor with hygroscopic sensing material (ANDIVI, 2020).

Referring to Figure 2.1.2 (c), resistive humidity sensors work by measuring changes in the electrical resistance of hygroscopic materials as they absorb water vapor from the surrounding environment. These materials rely on

their conductive properties, which change in response to the humidity. The relationship between relative humidity (RH) and resistance in resistive humidity sensors, as shown in Figure 2.1.2 (d), is typically inversely proportional – water molecules absorbed onto the sensing element reduce its resistance. This occurs because the water molecules dissociate the ionic functional groups on the material’s surface, enhancing conductivity through the donation of electrons (Ilmira et al., n.d.).

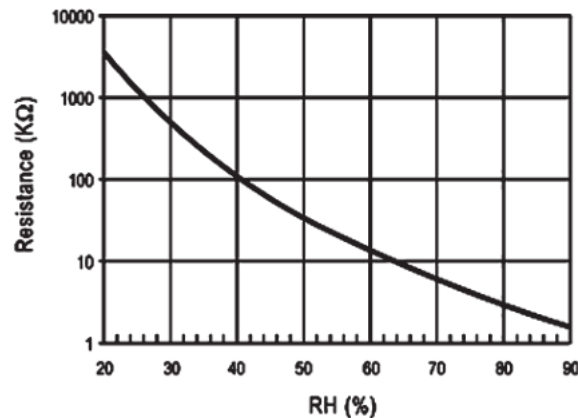


Figure 2.1.2 (d): Relationship of resistive change to humidity
(Sensor Technology Handbook, 2005).

The materials used for the sensing element in resistive humidity sensors are primarily categorized into ceramics, polymers, and electrolytes (Lee and Lee, 2005). Ceramic materials are favored for their excellent chemical and physical stabilities, ensuring reliable performance in various environments. Polymers, due to their ease of fabrication and tunable properties, offer flexibility and cost-effectiveness, making them an attractive option for large-scale production. Polymer electrolytes or polymer-salt complexes are also commonly employed, enhancing the ionic conductivity essential for humidity sensing (Burcu Arman Kuzubasoglu, 2022). In addition to these materials, thick-film technology is also frequently used for sensor fabrication. This technique supports efficient mass production while maintaining robustness and flexibility in sensor design.

The design of resistive humidity sensors closely resembles that of capacitive humidity sensors, with the key distinction being that conductivity-sensitive layers replace the dielectric layers. These sensors are characterized

by simple electrical circuits, high sensitivity, and good linearity, enabling accurate and easy calibration. Furthermore, they offer a wide operating range for both humidity and temperature, making them suitable for various industrial and environmental applications. However, resistive humidity sensors do have some limitations. Humidity hysteresis can be a significant issue, especially when the sensor is used intermittently. Additionally, the response time of resistive humidity sensors tends to be slower compared to other types of humidity sensors, and long-term stability is dependent on continuous operation and regular maintenance. Finally, resistive polymer-based sensors typically operate effectively with a narrower temperature range, generally between 0°C and 80°C (Ilmira et al., n.d.).

Several research studies have explored different materials and designs for resistive humidity sensors. A review by Lee and Lee (2005) states that a sensor using sensing film made from polyvinyl alcohol (PVA) and graphitized carbon black demonstrated sensitivity values of 8 ohm/%RH at room temperature and 5 ohm/%RH at 100°C. Another study involving Nafion, a polymer electrolyte, revealed that varying the ionic form of Nafion (H^+ , Li^+ , or Na^+) significantly impacted the sensor's performance. Furthermore, a sensor fabricated using poly-AMPS (poly(2-acrylamido-2-methylpropane sulfonate)) modified with TEOS (tetraethyl orthosilicate) exhibited reduced hysteresis ($< 2\%$) and high linearity ($R^2 = 0.9989$) across a wide humidity range (30% – 90% RH), showcasing good long-term stability and resistance to high humidity levels. Additionally, resistive sensors made from poly(N,N-dimethylpropargylamine) and poly(propargylalcohol) demonstrated measurable responses to relative humidity as low as 2%, with a broad dynamic range spanning from 0% – 90% RH. These studies illustrate the potential for further optimization of resistive humidity sensors in terms of sensitivity, stability, and response time.

Optical Humidity Sensor

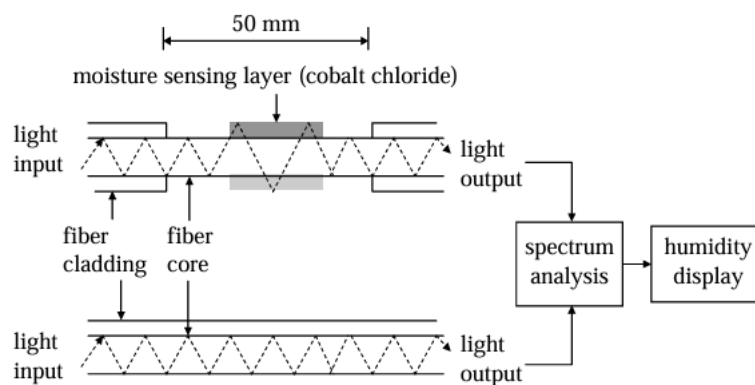


Figure 2.1.2 (e): Optical humidity sensor detects changes via cobalt chloride-gelatin film, with unmodified fiber as reference (Lee and Lee, 2005).

Optical humidity sensor shown in Figure 2.1.2 (e) utilize the colorimetric interaction of materials immobilized on the surface of the fiber core or its cladding to detect changes in relative humidity. These sensors rely on a sensing mechanism based on the humidity-induced refractive index change in the materials, which in turn alters the transmitted optical intensity through the sensing section. As the relative humidity changes, this variation in optical intensity can be correlated with the moisture content of the environment.

Several materials have been employed in optical humidity sensors to enhance their sensitivity and performance. From Lee and Lee (2005), cobalt chloride-gelatin thin films exhibit changes in spectral absorption in the wavelength range of 600 – 740 nm as the relative humidity fluctuates. Other materials, such as polyvinyl alcohol (PVA) doped with phosphoric acid (H_3PO_4) and dyes, show a notable shift in their spectrum when exposed to varying humidity levels. Additionally, phenol red-doped polymethylmethacrylate (PMMA) films, as well as nano-structured magnesium-oxide films, have been incorporated into the sensor design, capitalizing on their ability to interact with moisture and change the optical properties in response. These materials often offer high detection resolution, with some systems achieving sensitivity levels as precise as 0.56% RH.

The design of optical humidity sensors varies with key configurations incorporating fiber-optic technology, mechanical-optoelectronic systems, U-shaped probes, and photo-acoustic systems. Fiber-optic designs, such as those proposed by Kharaz and Jones (1995), often involve the modification of the fiber cladding. These sensors exploit the principle of light attenuation in optical fibers to quantify the moisture content. In mechanical-optoelectronic system, the sensor uses both fiber optics and a mechanical component to detect humidity. One example is a hair sensor, where the hair expands or contracts due to changes in moisture, moving a metal sheet or part of the sensor. This movement alters how much light passes through the fiber optics, which is then detected by a light sensor (LED and photodiode). The U-shaped probe design, as reported by Gupta and Ratnanjali (2001), uses a small portion of the core of a plastic-clad silica (PCS) fiber coated with a PMMA film. The bending of the fiber core within the probe enhances the interaction between the light and the sensing material, leading to improved sensitivity. Meanwhile, photo-acoustic humidity sensing systems, which utilize laser diodes, can detect water vapor concentrations at sub-ppm levels, offering ultra-sensitive detection ideal for precise moisture monitoring.

One of the primary advantages of optical humidity sensors is their high sensitivity, making them suitable for detecting low levels of moisture that other types of humidity sensors may overlook. Their inherent noise immunity and ability to transmit data over long distances – owing to the low attenuation of optical fibers – further enhance their applicability in diverse environments. These sensors also offer rapid response times, enabling real-time monitoring of relative humidity. Furthermore, optical humidity sensors are particularly well-suited for deployment in harsh environments, such as high-temperature or chemically corrosive industrial settings, where electronic or contact-based sensors often degrade or fail.

Nevertheless, despite their advantages, optical humidity sensors also face certain limitations. According to Lee and Lee (2005), hysteresis of the sensor can range from 0.5% to 1% RH, affecting measurement accuracy. Additionally, the bulky nature of some sensor designs, particularly those

involving large fiber-optic components or complex mechanical elements, can hinder their integration into compact systems. Optical humidity sensors also require frequent maintenance, such as mirror decontamination and temperature compensation mechanisms, to ensure consistent performance. The relative high-power consumption of some designs coupled with their high cost may also be a deterrent for certain commercial applications.

Overall, optical humidity sensors offer a high degree of sensitivity and reliability, making them invaluable in laboratory and specialized industrial environments.

Thermal Conductivity Humidity Sensor

Thermal conductivity humidity sensors are specialized devices designed to measure the absolute humidity of the surrounding air, making them particularly suitable for use in harsh or challenging environments. These sensors operate on the principle that the thermal conductivity of air varies with the amount of water vapor present. The sensor consists of two negative temperature coefficient (NTC) thermistor elements arranged within a bridge circuit as shown in the Figure below.

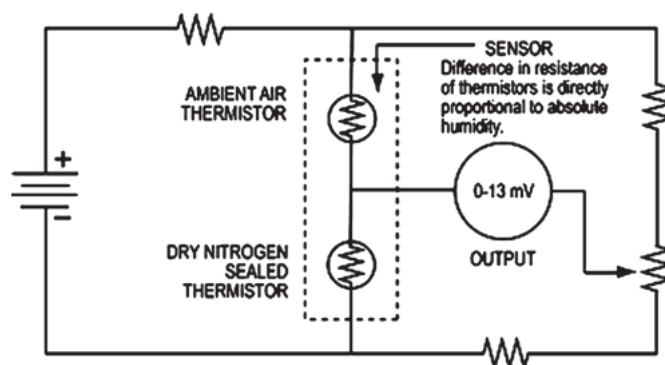


Figure 2.1.2 (f): Thermal Conductivity Humidity Sensor
(Sensor Technology Handbook, 2005).

One thermistor is sealed in dry nitrogen, acting as a reference element, while the other is exposed to the ambient air to detect changes in humidity. The measurement is based on the difference in thermal conductivity between the two thermistors. As the humidity in the surrounding air increases, the thermal conductivity of the exposed thermistors rises, altering its resistance.

This change in resistance is then measured and is directly proportional to the absolute humidity of the air.

These sensors are especially advantageous in environments with high temperatures or pollution. This makes them ideal for use in industries such as HVAC, environmental monitoring, and industrial processes where precise moisture control is critical. However, while thermal conductivity humidity sensors are highly durable, they can be sensitive to fluctuations in temperature, requiring careful calibration and maintenance to ensure accurate readings over time.

Hygrometers

Hygrometers are specialized instruments designed to measure the water content or absolute humidity in the air. These sensors offer precise measurements through various technologies, each suited for different applications. According to Chen and Lu (2005), the most common units of measurement used by hygrometers are Dew/Frost Point (D/F PT) and Parts Per Million (PPM), both of which indicate the amount of water vapor present in the air.

Hygrometers come in several types, each utilizing different principles to measure moisture. This review focuses on two primary types: mirror-based dew/frost point sensors and solid-state aluminum oxide moisture sensors. These technologies differ in their approach, cost, and accuracy.

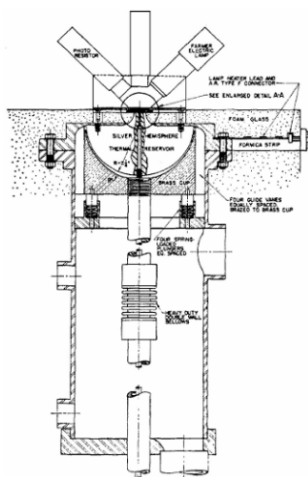


Figure 2.1.2 (g): Chilled mirror hygrometers (Chen and Lu, 2005).

Chilled mirror hygrometers are among the most accurate devices for measuring the dew or frost point, which reflects the temperature at which water vapor condenses on a mirror surface. The operating principle is based on detecting moisture condensation as the temperature of the mirror is lowered. As the mirror cools, water vapor from the surrounding air condenses when the temperature reaches the dew point, and this condensation is detected optically.

The structure of a chilled mirror hygrometer typically consists of a light source projected onto a sensing element (often a gold-coated mirror) and a photoresistor placed to detect changes in the optical signal as condensation forms on the mirror's surface. The temperature at which condensation occurs is recorded to determine the dew or frost point.

In recent years, various enhancements have been introduced to improve the performance of these sensors. For instance, optical fibers are sometimes used to separate the optical dew detector from the mirror surface, reducing the influence of the heating device and enhancing measurement accuracy. Additionally, some models employ laser light to detect dew formation through light scattering from a rough metal surface, achieving an accuracy of $\pm 0.5^\circ\text{C}$ in dew point detection. (Chen and Lu, 2005)

Chilled mirror hygrometers offer high accuracy and can measure absolute humidity even in extremely dry air. Enhancements like the integration of Peltier devices (thermoelectric coolers) and silicon dew point detectors have improved both the response time and stability of these sensors (Chen and Lu, 2005). Despite their advantages, chilled mirror hygrometers tend to be expensive due to their complex design. Besides, their mirror surface is prone to contamination, which can degrade measurement accuracy over time. Continuous use may also lead to instability, hence, demanding frequent calibration and maintenance.

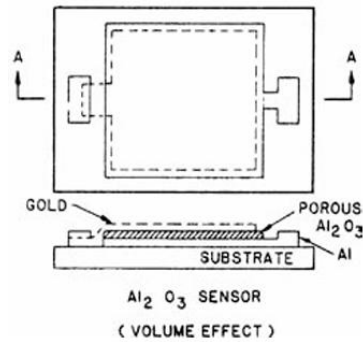


Figure 2.1.2 (h): Aluminum oxide moisture sensors (Chen and Lu, 2005).

Aluminum oxide moisture sensors represent an alternative technology for measuring humidity. These solid-state sensors operate based on a thin film of aluminum oxide (Al_2O_3), which detects water vapor in a gas. The sensor typically consists of a capacitor-like structure with an anodized porous aluminum oxide film and a water-permeable gold electrode. When water vapor interacts with the sensor, it passes through the gold electrode and is absorbed by the porous structure of the aluminum oxide film. This absorption alters the sensor's impedance, which is then measured to determine absolute humidity.

The primary advantage of aluminum oxide moisture sensors is similar to that of chilled mirror hygrometer: their ability to detect extremely low moisture levels, making them highly sensitive to humidity changes. They are relatively inexpensive to manufacture, which makes them ideal for large-scale deployment where cost is a critical factor. However, long-term instability remains a concern, as the sensor's performance can degrade over time due to factors such as contamination or material aging. While recent improvements in calibration techniques and materials have mitigated this issue, some users still face challenges with drift in sensor accuracy. Besides, while sensitivity to low moisture levels is an advantage, it can also lead to over-sensitivity in environments with fluctuating humidity.

Table 2.1.2: Overview of Different Types of Humidity Sensors.

Sensor Type	Operating Principle	Key Materials	Advantages	Limitations
Capacitive Humidity Sensor	Measures changes in capacitance due to variations in dielectric constant of hygroscopic material	- Polyimide films - PMMA-DVB - porous ceramics - porous silicon	- Low power consumption - Fast response time - High sensitivity - Reliable even at low RH	- Hysteresis - Temperature dependence - Nonlinear relationship
Resistive Humidity Sensor	Measures the change in electrical resistance as sensing material absorbs water vapor	- Ceramics - Polymers - Electrolytes	- Simple design - Good linearity - High sensitivity	- Hysteresis - Slower response time - Narrower temperature range
Optical Humidity Sensor	Measures changes in refractive index or optical intensity due to humidity-induced material changes	- Cobalt chloride-gelatin - PVA - phenol red-PMMA - Magnesium-oxide films	- High sensitivity - Noise immunity - Real-time monitoring - Rapid response	- Hysteresis - Complex design - High power consumption - Costly
Thermal Conductivity Humidity Sensor	Measures the difference in thermal conductivity of air with varying water vapor content	NTC thermistors	- Highly durable - Suitable for harsh environments - Precise absolute humidity measurement	- Sensitive to temperature fluctuations - Requires calibration
Hygrometer (Chilled Mirror)	Detects condensation on a mirror surface as the temperature drops to dew point	- Gold-coated mirror - Photoresistor	- High accuracy - Can measure absolute humidity even in dry air	- Expensive - Prone to contamination - Requires frequent maintenance
Hygrometer (Aluminium Oxide)	Measure impedance changes as water vapor interacts with aluminum oxide film	- Aluminum oxide - Gold electrode	- Sensitive to low moisture levels - Cost-effective	- Long-term instability - Drift in sensor accuracy over time

An overview of the types of humidity sensors discussed in this subsection is provided in Table 2.1.2. Understanding the different types of humidity sensors and their respective characteristics is essential for selecting the most suitable sensor for specific applications. With advancements in sensor technologies, their importance continues to grow across various fields.

2.1.3 Importance of Humidity Sensor

Humidity sensors play a crucial role in providing accurate and real-time monitoring of moisture levels in the environment. Their versatility and accuracy make them critical for ensuring quality, safety, and efficiency in a broad range of applications. For example, maintaining optimal conditions in industrial processes, environmental systems, healthcare, agriculture, and beyond.

i. Industrial Applications

In industrial settings, humidity sensors are vital for maintaining controlled environments necessary for manufacturing and production processes. For instance, in the production of semiconductors, electronics, and pharmaceuticals, even minor deviations in humidity can compromise product quality. Similarly, in industries such as food

and beverage, cosmetics, and biomedical products, humidity control is vital for preserving product integrity and ensuring compliance with safety standards. These sensors are also integral to drying processes in industries like paper, textile, and wood, where precise moisture levels are required to achieve desired material properties. By enabling real-time process monitoring, humidity sensors help optimize production efficiency and reduce waste.

ii. Environmental Control and Monitoring

Humidity sensors are key components in building management systems, where they regulate heating, ventilation, and air conditioning (HVAC) systems to maintain comfortable and energy-efficient indoor environments. They are also used in environmental chambers to prevent issues such as mold growth and to test the durability and performance of electronics and other equipment under controlled conditions. In meteorological applications, humidity sensors are essential for weather stations, providing data for accurate weather forecasting and climate analysis. This information is crucial for disaster preparedness, agriculture, and urban planning.

iii. Agriculture Optimization

In agriculture, humidity sensors contribute significantly to optimizing crop growth and resource management. By monitoring soil moisture levels, these sensors help farmers implement precise irrigation strategies, reducing water waste and enhancing crop yields. In greenhouses, humidity sensors help regulate temperature and moisture levels to ensure optimal growth conditions for plants. They are also used in the storage of grains and cereals, where maintaining proper humidity levels prevents spoilage and preserves product quality.

iv. Healthcare and Medical Applications

The healthcare sector relies heavily on humidity sensors for various critical applications. These sensors are used in medical devices such as respiratory equipment, incubators, and sterilization systems, where

maintaining specific humidity levels is essential for patient safety and effective treatment. Humidity sensors also play a role in diagnosing respiratory conditions like asthma and sleep apnea, as well as monitoring breathing patterns in real-time. Furthermore, advancements in wearable technology – such as smartwatches, fitness trackers, and bio-sensing patches – have led to the integration of flexible humidity sensor into devices that track skin moisture, sweat, and respiration, offering new possibilities for personalized healthcare and wellness monitoring.

v. Automotive and Safety Applications

In the automotive industry, humidity sensors are utilized in applications like rear-window defoggers and motor assembly lines, where controlling moisture levels ensures safety and operational efficiency. Beyond automotive uses, these sensors are also crucial for safety monitoring in various settings. For example, they can detect unsafe moisture levels in electrical equipment, preventing potential hazards, or identify leaks in pipelines, helping to mitigate damage and resource loss.

vi. Consumer and Household Applications

Humidity sensors are increasingly being integrated into smart appliances such as microwave ovens, refrigerators, and clothes dryers, enhancing their functionality and energy efficiency. They also play a crucial role in food storage and transportation, ensuring that perishable goods remain fresh and safe for consumption. Emerging applications, such as smart wearables and non-contact sensors for skincare, demonstrate the expanding potential of humidity sensors in innovative and consumer-focused technologies.

By enabling real-time humidity measurement and control, these sensors help prevent material degradation, improve energy efficiency, enhance process reliability, and contribute to advancements in smart technologies.

2.1.4 Limitations of Conventional Humidity Sensors

As the demand for precise and adaptive humidity sensing continues to grow, the development of more efficient and versatile sensor technologies remains essential. However, despite their numerous advantages, conventional humidity sensors face certain limitations that can affect their long-term performance and applicability.

One of the most significant challenges is their power dependency. Most traditional humidity sensors, especially those based on capacitive, resistive, or optical principles, require an external power source to operate. This reliance on continuous power can be problematic in remote or hard-to-reach locations where the energy supply is either limited or unavailable. In such cases, the need for external power sources increases the overall system complexity and operational cost, making these sensors less ideal for sustainable and long-term monitoring solutions.

Moreover, the integration of conventional humidity sensors into portable or miniaturized devices often results in challenges related to size, weight, and energy efficiency. These sensors, when designed for low-power consumption, may sacrifice sensitivity and response time, further limiting their use in applications requiring rapid and accurate humidity measurements. As a result, conventional sensors often struggle to meet the demands of modern applications that require high precision, reliability, and low maintenance – particularly in energy-constrained systems.

These limitations underscore the need for innovative solutions in the field of humidity sensing. The inherent drawbacks of conventional sensors have driven significant research into the development of self-powered sensors.

2.2 Self-Powered Sensors

The concept of self-powered sensors represents a paradigm shift in the design and deployment of sensor technologies, particularly within the context of the Internet of Things (IoT) and sustainable development. Unlike conventional sensors that rely on batteries or external power supplies, self-powered sensors are engineered to function autonomously by harvesting energy from their surrounding environment. This approach not only reduces dependence on finite power sources but also addresses the limitations associated with battery-powered system, such as restricted lifespan and the need for regular maintenance or replacement.

2.2.1 Relevance in the Era of IoT

In the context of IoT, where the vision of a “Trillion Sensor Universe” is becoming increasingly tangible, the scalability of sensor deployment presents significant challenges (Akinaga, 2020). The traditional reliance on batteries becomes impractical when considering the deployment of billions or trillions of sensors across various environments, including remote and inaccessible areas. Battery replacement or recharging in such scenarios is not only labor-intensive and costly but often technically unfeasible. Self-powered sensors, by eliminating the need for external power sources, enable large-scale and long-term deployment of wireless sensing networks, making them a critical enabler of IoT applications in environmental monitoring, smart agriculture, industrial automation, and wearable electronics.

2.2.2 Role in Promoting Sustainable Technology

Beyond technical convenience, self-powered sensors also align with global efforts to promote sustainable and energy-efficient technologies. As concerns about the depletion of non-renewable energy sources and environmental sustainability grow, the need for systems that utilize renewable and ambient energy has become increasingly urgent. Self-powered sensors support the goal of ensuring access to affordable, reliable, sustainable, and modern energy systems. By utilizing energy that would otherwise go to waste, these systems reduce environmental impact, extend device lifespans, and contribute to the development of more sustainable technological ecosystems.

2.2.3 Mechanisms of Energy Harvesting in Self-Powered Sensor Technology

This subsection provides an overview of the key energy harvesting techniques that form the foundation of modern self-powered sensor systems.

Solar Energy Harvesting

Solar energy harvesting, primarily through photovoltaic (PV) cells, remains one of the most established methods for generating electricity from the environment. PV cells convert sunlight – comprising electromagnetic radiation in the visible spectrum – into electrical energy. Outdoor sunlight can provide up to 100 mW/cm^2 , while indoor lighting offers significantly lower, yet still usable, power levels of approximately $100 \text{ }\mu\text{W/cm}^2$. These outputs are typically sufficient for low-power electronic devices. Solar-based energy harvesting has been applied in technologies such as solar windows, lightweight PV cells, and smart wallpaper (Sil, Mukherjee and Biswas, 2017). Ongoing research focuses on developing flexible solar cell arrays suitable for integration into wearable and biomedical devices. However, Figure 2.2.3 (a) and Figure 2.2.3 (b) showed that the relatively larger size of photovoltaic harvesters may pose limitations for miniaturized applications when compared to piezoelectric and thermoelectric alternatives.

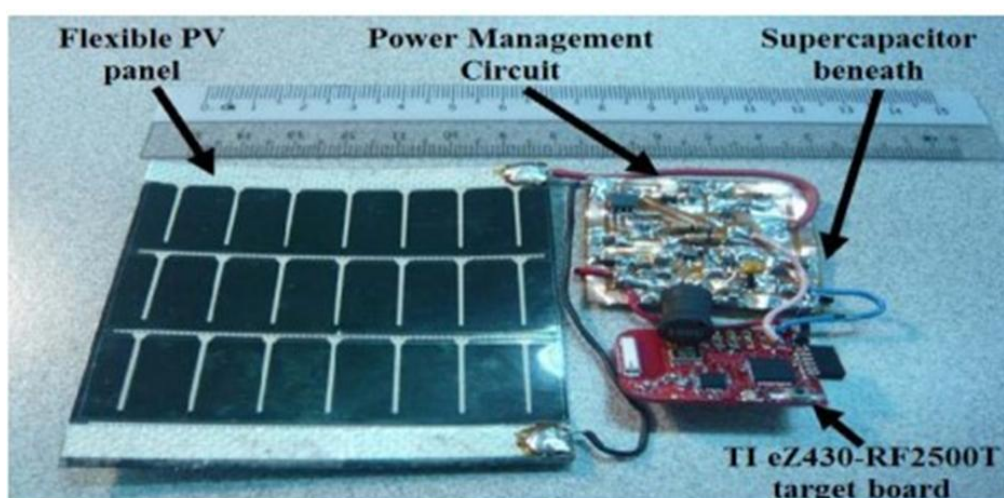


Figure 2.2.3 (a): Flexible solar-based wearable energy harvester (Toh et al., 2014).

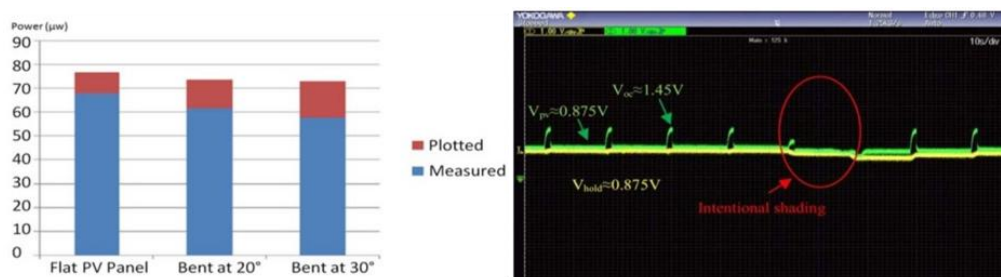


Figure 2.2.3 (b): (left) Measured output of flexible PV panel. (right) Flexible PV panel voltage with MPPT control under a lighting intensity of 320 lux.

(Toh et al., 2014)

Piezoelectric Energy Harvesting

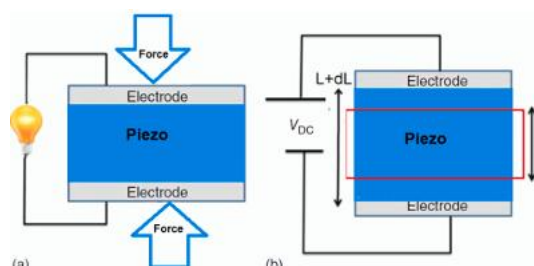


Figure 2.2.3 (c): Schematic sketch of direct (a) and indirect (b) piezoelectric effects (Ali et al., 2019) .

Piezoelectric energy harvesting shown in Figure 2.2.3 (c) is a widely studied method for converting mechanical vibrations into electrical energy, making it particularly effective in environments with consistent or repetitive motion. The working principle is based on the piezoelectric effect, wherein mechanical stress or strain applied to certain dielectric materials induces dielectric polarization, resulting in surface charges accumulation and an associated electric potential. Materials such as lead zirconate titanate ($Pb[Zr, Ti]O_3$ or PZT) exhibit high energy conversion efficiency and have been extensively utilized (Akinaga, 2020). According to Ali et al. (2019), ongoing research is also exploring lead-free alternatives and flexible organic materials, such as polyvinylidene fluoride (PVDF), its copolymer P(VDF-TrFE), and bio-based piezoelectric materials like diphenylalanine (FF).

Piezoelectric nanogenerators (PNGs), which leverage nanostructured materials to harvest biomechanical energy from sources such as body movements, blood flow, cardiac motion, and lung activity, are being developed for biomedical applications, including self-powered implantable medical devices. These systems are especially well-suited for wearable electronics and health-monitoring devices, where mechanical energy from everyday human activity (e.g., walking or breathing) can be harnessed to sustain device functionality.

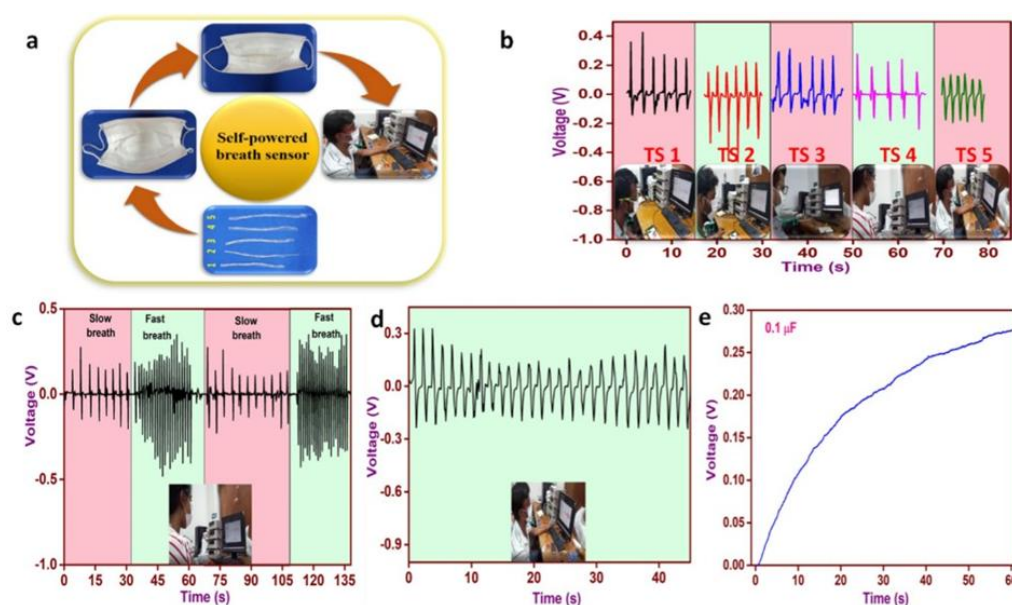


Figure 2.2.3 (d): (a) Application of self-powered respiratory sensor in face-mask. (b) Output voltage upon slow inhale/exhale conditions of five different candidates. (c) Output voltage upon slow and fast inhale/exhale conditions of the same candidates. (d) Stable output voltage response over a period of time. (e) Charging of 0.1 μF capacitor using the output voltage upon continuous inhale/exhale (Raj et al., 2018).

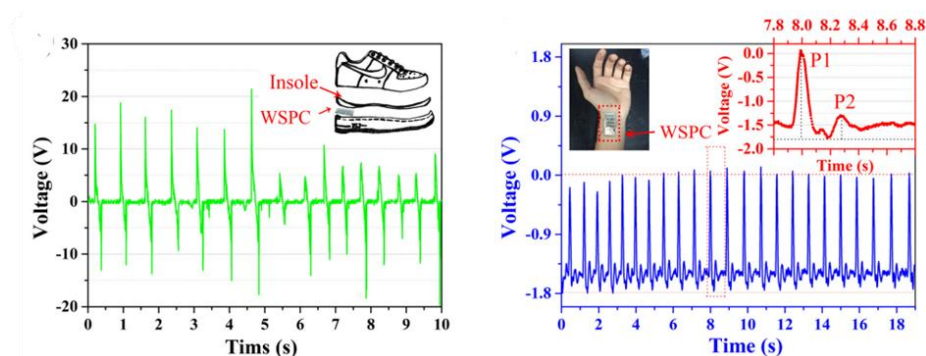


Figure 2.2.3 (e): (left) Output voltage during walking. (right) Voltage output of human pulse test (You et al., 2016).

Thermoelectric Energy Harvesting

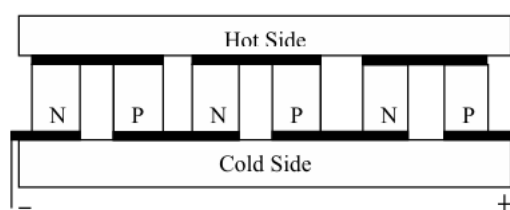


Figure 2.2.3 (f): Schematic sketch of thermoelectric generators (Sil, Mukherjee and Biswas, 2017).

Thermoelectric energy harvesting involves converting heat differentials into electrical energy through the Seebeck effect. When a temperature gradient exists across a thermoelectric material, a voltage is generated proportional to the temperature difference. This technique is particularly valuable in environments where waste heat is abundant, such as industrial settings or from the human body. The efficiency of thermoelectric materials is measured by the figure of merit, which depends on the Seebeck coefficient, electrical conductivity, thermal conductivity, and operating temperature.

While conventional metallic thermoelectric materials exhibit limited efficiency, ongoing research focuses on advanced materials such as silicon-based compounds, carbon nanotube thin films, and flexible organic composites that are more suitable for wearable applications (Akinaga, 2020). Sil, Mukherjee and Biswas (2017) states that thermoelectric generators (TEGs) are already in use for powering small-scale electronics by harvesting heat from machinery, vehicles, or even body heat in wearable and medical devices.



Figure 2.2.3 (g): Pulse oximeter powered by watch-style thermoelectric generator (Ghomian and Mehraeen, 2019).

Triboelectric and Electrostatic Energy Harvesting

Triboelectric and electrostatic energy harvesting techniques generate electrical charge through friction contact or mechanical displacement. In triboelectric nanogenerators (TENGs), energy is harvested via contact and separation between materials with different electron affinities, producing charge through the triboelectric effect. TENGs have shown significant promise in capturing biomechanical energy, airflow, and structural vibrations (Figure 2.2.3 (h)) for use in self-powered sensor systems.

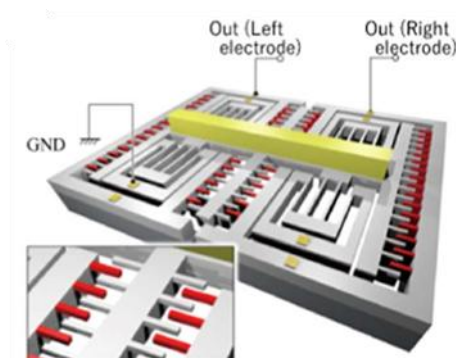


Figure 2.2.3 (h): MEMS vibrational energy harvester (Akinaga, 2020).

Electrostatic energy harvesting, by contrast – including electret-based systems – relies on variations in capacitance caused by mechanical vibrations to generate electrical energy. These systems often incorporate microelectromechanical systems (MEMS) technologies, such as comb electrodes and voltage-boost rectifiers, to enhance efficiency (Akinaga, 2020). Electrostatic harvesters are particularly effective for harvesting low-frequency vibrations and are well-suited for miniaturized applications.

Electromagnetic Energy Harvesting

Electromagnetic energy harvesting is based on Faraday's law of electromagnetic induction, which states that a changing magnetic field within a coil induces an electric current. This technique is commonly used in environments with persistent mechanical vibrations, such as transportation systems and industrial machinery. Devices employing this method convert kinetic energy into electrical power using magnetic components and are often integrated into hybrid systems alongside other energy harvesting techniques to enhance overall performance.

Wind Energy Harvesting

Wind energy harvesting is a viable source of ambient energy, capable of providing power densities of approximately $100 \mu\text{W}/\text{cm}^3$. At the microscale, wind energy is typically captured using mechanical systems such as micro-turbines or flutter-based devices. While large-scale wind power generation (e.g., conventional wind turbines) lies outside the scope of most self-powered sensor applications, small-scale wind harvesting is particularly useful for powering remote wireless sensors, especially in outdoor or isolated environments.

2.2.4 Limitations of Current Self-Powered Technologies

Despite significant advancements in energy harvesting technologies, current self-powered systems face several critical limitations that hinder their broader deployment. Most conventional energy harvesting mechanisms are constrained by their reliance on specific environmental conditions, limiting their effectiveness across diverse real-world scenarios. For example, piezoelectric and triboelectric systems require consistent mechanical motion or vibration, making them ineffective in static or low-movement environments. Thermoelectric generators depend on a stable and substantial temperature gradient, which is often unsustainable in portable or wearable contexts. Similarly, solar harvesters are highly dependent on light intensity and orientation, with their performance significantly reduced under low-light or indoor conditions. Wind and electromagnetic energy harvesters typically require bulky or complex setups, making them less suitable for compact, wearable, or implantable systems.

Furthermore, material limitations and integration challenges persist across many of these technologies. Rigid structures, limited mechanical durability, and complex fabrication process can hinder the development of flexible, biocompatible, and cost-effective devices – particularly for wearable and implantable applications. Certain materials, such as lead-containing piezoelectric ceramics, pose environmental and health risks, while others involve trade-offs between energy conversion efficiency and mechanical performance. Additionally, scalability and miniaturization remain significant

barriers, as many energy harvesting systems cannot be efficiently reduced to the microscale without compromising power output.

In light of these challenges, there is growing interest in exploring alternative energy harvesting strategies that are environmentally benign, mechanically flexible, scalable, and capable of operating under a wider range of ambient conditions. One such approach is Moisture-induced Electricity Generation (MEG).

2.3 Moisture-Induced Electricity Generation

Moisture-induced electricity generation (MEG) is an emerging clean energy-harvesting technology that converts the ubiquitous presence of atmospheric water – particularly water vapor and ambient moisture – into electrical energy. Unlike conventional energy harvesting methods, MEG leverages interactions between water molecules and functional materials at the solid-water interface to generate electricity, without requiring external stimuli such as temperature gradients, mechanical motion, or light exposure. Given that atmospheric moisture is one of the most abundant and renewable natural resources on Earth, MEG offers a highly eco-friendly and potentially scalable solution for powering low-energy electronic devices, especially in environments where other ambient energy sources are limited. This approach represents a new frontier in hydrovoltaic technology, shifting the focus from liquid water-based systems to harnessing the often-overlooked potential of gaseous water molecules in the atmosphere.

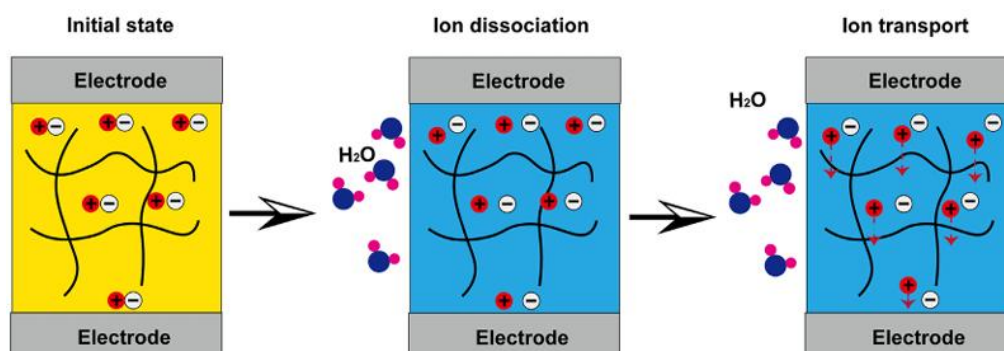


Figure 2.3: Schematic mechanism of MEG (Sun et al., 2022).

2.3.1 Mechanisms Used for MEG

Ion diffusion

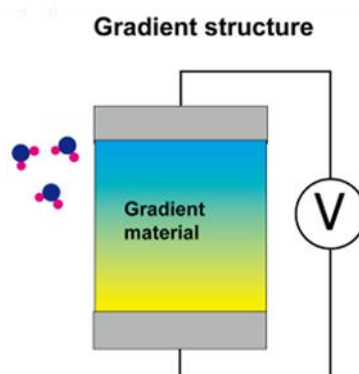


Figure 2.3.1 (a): MEG using gradient material (Sun et al., 2022).

The mechanism of MEG involves several key physical and chemical processes occurring at the water-solid interface. One of the most studied is ion diffusion, also referred to as ion-gradient-driven electricity generation. This process relies on hygroscopic materials – often polymers or porous solids – bearing functional groups such as $-\text{OH}$, $-\text{COOH}$, or $-\text{SO}_3\text{H}$. These groups interact with adsorbed water molecules and ionize, releasing mobile ions. When structural or chemical asymmetry exists – whether due to variations in material composition, moisture distribution, or layered geometry – a concentration gradient is formed, which drives the directional migration of ions. This ion movement generates an internal electric field, resulting in a measurable voltage output between electrodes. The duration and magnitude of power generation are influenced by the material's ion-release capacity and the stability of the moisture gradient.

Streaming potential

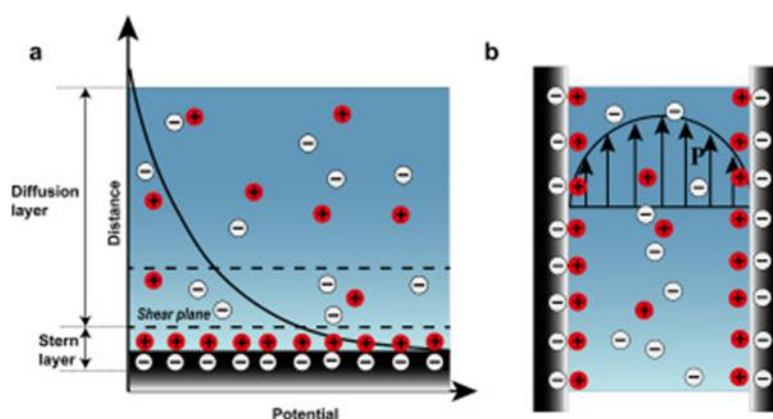


Figure 2.3.1 (b): (a) Schematic representation of the electric double layer forming at the solution–solid interface. (b) Schematic depiction of the classical electrokinetic effect within a nanochannel. (Sun et al., 2022)

Another mechanism underlying MEG is the streaming potential, commonly observed in nanochannels. When a charged solid surface comes into contact with moisture, it forms an electric double layer (EDL) – consisting of a layer of immobile surface charges and a surrounding layer of mobile counterions in the water (Sun et al., 2022). As moisture flows through or along the channel, it transports these mobile ions, generating a current known as the streaming current, and a corresponding voltage referred to as the streaming potential. This mechanism is highly influenced by factors such as surface charge density, channel dimensions, material wettability, and fluid dynamics, and has been effectively utilized in nanoscale MEG devices.

Charged surface potential

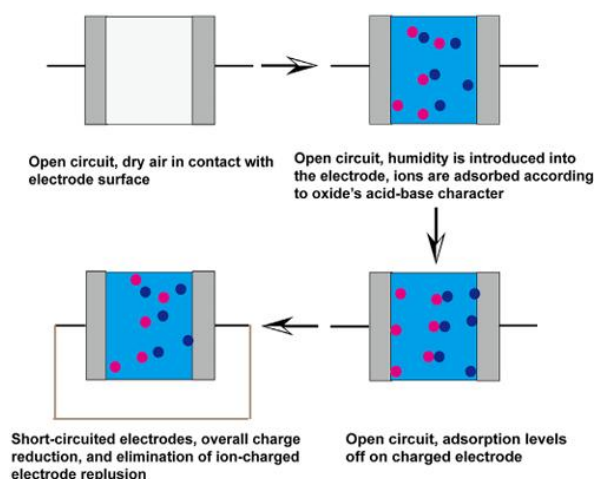


Figure 2.3.1 (c): Charge build-up and discharge of electrodes in a capacitor

(Sun et al., 2022).

A third mechanism involves charged surface potential, wherein certain metals accumulate charge upon exposure to humidity through the selective adsorption of water-derived ions such as H^+ and OH^- (Sun et al., 2022). When two different metals with distinct adsorption characteristics are placed in a humid environment and separated by a dielectric layer, a potential difference is generated due to unequal charge accumulation. This asymmetric configuration functions analogously to a self-charging capacitor, offering an alternative pathway for electricity generation without requiring ion flow or fluidic channel structures.

Together, these diverse yet complementary mechanisms – ion diffusion, streaming potential, and charged surface interaction – form the scientific foundation of MEG. With ongoing advances in materials science and device engineering, MEG systems have progressed from generating millivolt-scale outputs to delivering several volts per device, with sufficient capacity to power small electronic systems. As a result, MEG holds great promise as a next-generation sustainable power solution, particularly for autonomous sensors and Internet of Things (IoT) applications in environments with consistent ambient humidity.

2.3.2 Materials Used for MEG

The performance and operating principles of MEG devices are strongly influenced by the choice of materials, as these determine how moisture interacts with the system and how effectively charge carriers are generated and transported. Various categories of materials have been explored for their distinct physicochemical properties, each enabling different MEG mechanisms.

Carbon-based materials

Carbon-based materials, particularly graphene and its derivatives, are among the most extensively studied for MEG applications. Graphene oxide (GO) is especially attractive due to its high surface area and abundance of oxygen-containing functional groups, such as hydroxyl ($-OH$) and carboxyl ($-COOH$). These groups facilitate the rapid adsorption and desorption of water molecules, weakening hydrogen bonds and releasing free protons. The migration of these protons across the material establishes a concentration gradient, which drives ion diffusion-based electricity generation. Although early GO-based MEG devices produced only transient outputs due to rapid dissipation of the gradient, Shen et al. (2020) stated that recent advances in structural design – such as gradient-controlled film layering – have enabled continuous voltage generation over extended periods.

Other carbon-based materials, including carbon black (CB), carbon nanotubes (CNTs), and carbon dots, have also demonstrated MEG activity. According to the article, functionalized CNT films with asymmetric surface chemistries can induce proton-driven ion diffusion, while CB-based systems utilize streaming current mechanisms facilitated by water flow through carbon-rich channels.

Biomaterials

Biomaterials offer an eco-friendly and sustainable alternative for MEG applications. Materials such as cellulose and proteins naturally possess functional groups ($-OH$, $-COOH$, $-NH_2$) that facilitate strong interactions with moisture. These interactions can induce either streaming currents or ion diffusion, depending on the material's structure and the mobility of water

molecules. Biofibers extracted from sources like cellulose, chitin, or silk often carry surface charges, and when water moves through their porous networks, electricity is generated via electrokinetic streaming effects.

Particularly noteworthy are protein nanowires – such as those derived from *Geobacter sulfurreducens* – which have demonstrated long-lasting power output through self-sustained moisture gradients that derive continuous ion diffusion (Shen et al., 2020). Paper-based devices, rich in cellulose, typically produce transient outputs due to rapid water saturation and the collapse of the moisture gradient but remain useful for disposable or short-term applications.

Polymers

Polymers have gained increasing attention in MEG research due to their lightweight, flexible, and chemically tunable properties. Functional polymers such as Nafion, polyethersulfone (PES), and polyetherketone (PEK) exhibit good proton conductivity and contain hydrophilic groups that facilitate water uptake and subsequent proton release (Shen et al., 2020). These materials typically operate through ion diffusion, where moisture triggers charge separation and directional ion migration.

Conductive polymers like polypyrrole (PPy) introduce an additional layer of functionality, as internal anion gradients can enhance moisture-activated ion transport (Sun et al., 2022). Composite polymer structures that combine hydrophilic and conductive components have demonstrated improved performance across a broader range of humidity and temperature conditions. Furthermore, naturally derived polymers such as gelatin also exhibit MEG behavior through the formation of hydrogen-bonded water chains that support proton hopping, driven by the self-ionization of water.

Inorganic Semiconductor Materials

Inorganic semiconductor materials – particularly those engineered at the nanoscale – have been explored for MEG applications due to their ability to interact with water through surface electrokinetic effects. Nanowire networks of titanium dioxide (TiO₂), silicon (SiNWs), and other metal oxides

can generate streaming potentials as protons or cations in the adsorbed water layer migrate through nanochannels. The wettability, surface charge (zeta potential), and geometry of these nanostructures are critical parameters influencing device performance.

A wide range of metal oxides – including Al_2O_3 , Fe_2O_3 , Mn_3O_4 , ZnO , CuO , SnO_2 , and Fe_3O_4 – have demonstrated MEG potential through mechanisms such as water evaporation-induced charge separation or moisture-driven surface ion transport, thereby expanding the library of functional materials for device design (Shen et al., 2020).

In summary, the wide variety of materials explored for MEG reflects the multidisciplinary efforts to enhance energy harvesting through different operational mechanisms. Among these, carbon-based materials such as graphene oxide (GO) and carbon nanotubes (CNTs) have attracted considerable attention due to their tunable surface chemistry and interaction with moisture. However, challenges such as transient output stability and fabrication complexity remain. The fabrication of these materials often involves complex chemical synthesis routes, requiring multiple processing steps, hazardous reagents, or high-temperature treatments, which can limit scalability and increase production cost. In response to these limitations, recent studies have introduced laser-induced graphene (LIG) as a promising alternative, offering a scalable and controllable method to engineer graphene-like surfaces for MEG applications.

2.4 Laser-Induced Graphene

Laser-Induced Graphene (LIG) is a form of graphene synthesized through the direct laser irradiation of carbon-rich materials. In this method, a laser beam is used to locally heat and carbonize a precursor substrate – typically a synthetic polymer – resulting in the formation of a porous, three-dimensional graphene network. This process, often referred to as laser scribing or laser direct writing, is notable for being rapid, single-step, and mask-free, eliminating the need for additional reagents, catalysts, or complex patterning procedures.

Unlike conventional graphene synthesis techniques such as chemical vapor deposition or chemical exfoliation, LIG fabrication does not require high-temperature furnaces or hazardous chemicals. As a result, it offers a cost-effective, scalable, and environmentally friendly approach to graphene production.

A key feature of LIG is its versatility in terms of substrate compatibility. In addition to synthetic polymer, LIG has been successfully produced on a wide range of carbon-containing materials, including biodegradable and natural substrates (Moon and Ryu, 2024). This adaptability not only enhances the sustainability of the process but also enables the development of flexible, wearable, or biodegradable electronic devices. The resulting LIG material typically exhibits high electrical conductivity, mechanical flexibility, and chemical stability, making it well-suited for applications in sensors, energy storage devices, supercapacitors, and environmental monitoring technologies.

2.4.1 Historical Background

The foundation for graphene research was established with the isolation of monolayer graphene by Novoselov (2004), an achievement that earned them the Nobel Prize in Physics in 2010. However, the specific technique of Laser-Induced Graphene emerged a decade later. In 2014, a major breakthrough was reported by James M. Tour's research group at Rice University, which successfully synthesized 3D porous graphene structures from commercial polyimide (PI) films using a CO₂ infrared laser. This method enabled the localized photothermal conversion of PI into graphene under ambient conditions, and the resulting material was termed Laser-Induced Graphene (LIG). The technique quickly attracted attention for its simplicity and effectiveness.

The original demonstration by Lin et al. (2014) marked a new era in graphene fabrication, showcasing that laser scribing could be used not only to synthesize graphene but also to pattern it directly into device-relevant architectures. Since then, numerous studies have expanded upon this technique,

refining parameters such as laser wavelength, power, scanning speed, and precursor chemistry to optimize the structure, conductivity, and functional properties of LIG. As a result, LIG has become a widely studied material, particularly in applications requiring low-cost, flexible, and scalable nanomaterials.

2.4.2 Mechanism of Laser-Induced Graphene Formation

The formation of Laser-Induced Graphene (LIG) is primarily governed by laser ablation, which initiates both photothermal and photochemical transformations in carbon-rich precursor materials. These sections outline the underlying physical and chemical mechanisms of LIG synthesis, with a focus on laser-material interactions, the roles of thermal and photonic energy, and the influence of precursors composition and laser parameters on the structural and functional properties of the resulting graphene.

LIG formation is driven by a localized, laser-induced pyrolysis. When a focused laser beam irradiates the surface of a carbon-rich polymer such as polyimide (PI), the absorbed laser energy is converted into thermal energy, causing rapid and intense localized heating. This thermal effect decomposes (pyrolyzes) the polymer in an oxygen-limited environment, breaking molecular bonds and releasing volatile compounds, particularly those containing hydrogen, oxygen, and nitrogen.

The remaining carbon atoms undergo reorganization into sp^2 -hybridized graphitic domains, forming a 3D porous graphene network (Pinheiro et al., 2024). This transformation involves both aromatization and condensation reactions, through which disordered carbon transition into more ordered, hexagonally arranged graphene-like structures. The evolution of volatile gases during pyrolysis contributes to the expansion and porosity of the LIG material, resulting in its characteristic foam-like architecture.

2.4.3 Influence of Material Precursors and Laser Parameters

The efficiency and quality of LIG formation are highly dependent on both the chemical nature of the precursor material and the laser processing parameters.

According to Hong et al. (2023), polyimide (PI) is the most widely used precursor due to its high thermal stability, aromatic ring structures, and rich carbon content. The imide functional groups and charge-transfer complexes within PI facilitate graphitization when exposed to high temperatures. Upon laser irradiation, PI undergoes bond cleavage, leading to the release of gases such as H₂O, CO, CO₂, and NH₃, while the residual carbon reorganizes into porous graphene structures. In contrast, non-aromatic and natural substrates – such as wood, paper, coconut shell, cloth, and certain food items – can also be converted into LIG, although they may require surface modification strategies to enhance graphitization (Pineiro et al., 2023). For example, the application of fire retardants or pre-coating with carbon-rich layers can improve thermal stability and promote uniform carbonization in lignocellulosic substrates.

A wide range of laser parameters can be tuned to control the morphology, composition, and electrical properties of LIG. Table 2.4.3 outlines the following key parameters:

Table 2.4.3: Key Laser Parameters Affecting LIG Formation.

Parameters	Elaboration
Laser power and fluence (energy per area)	Critical for determining whether photothermal or photochemical processes dominate.
Scan speed and exposure time	Affect the duration of energy input and the degree of thermal accumulation.
Wavelength	Influences laser penetration depth and the material's absorption characteristics.
Pulse repetition frequency (PRF) and pulse duration (PW)	Shorter pulses reduce thermal damage and allow high-resolution patterning; longer pulses enhance thermal diffusion.
Defocus distance (z-position)	Alters the beam spot size and fluence, influencing pattern resolution and heat distribution.

By carefully optimizing these parameters, researchers can tailor the pore size, thickness, degree of graphitization, and electrical conductivity of LIG for specific applications. For instance, high laser power can promote deeper carbonization but may also risk damaging the substrate if not properly controlled, whereas lower power may improve resolution but result in incomplete conversion.

2.5 Summary

This chapter has reviewed existing literature relevant to the development of humidity sensors, with particular emphasis on the transition from conventional sensor systems to next-generation self-powered technologies. The discussion began with an overview of humidity sensing fundamentals, including key definitions, classifications, and performance parameters. The main types of humidity sensors – capacitive, resistive, optical, thermal conductivity, and hygrometric – were examined in detail, highlighting their operating principles, material compositions, advantages, and limitations. While each sensor type offers specific benefits, conventional systems are generally constrained by their reliance on external power sources, limited adaptability to environmental conditions, and challenges in long-term deployment.

In light of these limitations, the review turned toward the development of self-powered sensors – devices capable of harvesting ambient energy from their surroundings, thereby eliminating the need for continuous external power. Various energy harvesting strategies were explored, including photovoltaic, piezoelectric, thermoelectric, triboelectric, and electromagnetic methods. Although promising, these approaches face critical challenges such as environmental dependency, device bulkiness, material toxicity, and scalability concerns – especially when applied to flexible, miniaturized, and wearable devices.

To address these challenges, moisture-induced electricity generation (MEG) has emerged as a promising alternative. MEG systems exploit the ubiquitous presence of atmospheric moisture to generate electricity through mechanisms such as ion diffusion, streaming potential, and surface charge interactions. These mechanisms rely on moisture-responsive materials capable of sustaining directional ion transport or charge separation under ambient humidity conditions. A wide range of materials have been investigated for MEG applications, including carbon-based nanomaterials (e.g., graphene oxide and carbon nanotubes), biomaterials (e.g., cellulose and protein nanowires), functional polymers (e.g., Nafion), and inorganic semiconductors (e.g., metal oxides and nanowires).

The chapter also highlighted the potential of laser-induced graphene (LIG) as a scalable and efficient material platform for MEG-based sensor fabrication. LIG enables the rapid, cost-effective, and environmentally friendly production of porous graphene structures directly from carbon-rich substrates via laser irradiation. Its high conductivity, tunable morphology, and compatibility with flexible substrates make it especially well-suited for self-powered humidity sensors.

In summary, the literature supports the feasibility of developing a self-powered flexible humidity sensor by integrating MEG mechanisms with LIG-based materials. Such an approach addresses the key limitations of conventional humidity sensors and aligns with the current trends in sustainable, autonomous sensing technologies for Internet of Things (IoT) and wearable applications.

CHAPTER 3

METHODOLOGY AND WORK PLAN

3.1 Introduction

This chapter outlines the procedures used in the fabrication of a self-powered flexible humidity sensor based on moisture-induced electricity generation (MEG). The approach integrates a sustainable, low-power laser scribing technique to convert lignin-coated filter paper into a conductive sensing platform.

Unlike conventional methods that require high-energy CO₂ lasers, this study employs a more energy-efficient NEJE DK-8-KZ laser engraver operating at a wavelength of 405 nm. This approach significantly reduces power consumption and environmental impact while enhancing recyclability of materials. By utilizing simple, low-cost components such as paper, borax, boric acid, and lignin, this methodology offers a green and scalable route toward the development of MEG-based humidity sensors.

3.2 Equipment and Materials

The fabrication process employed a combination of laboratory tools, consumables, and chemicals, as detailed below:

Item description	*Item category	Quantity
Cellulose filter paper (Whatman paper grade 40)	C	1 box
Borax	CH	2.5 g
Boric acid	CH	2.5 g
Distilled water	C	100 ml
Lignin	CH	0.8 g
Hydroxyethyl cellulose (HEC)	CH	0.1 g
Beaker	W	2
Stainless steel laboratory spatula	W	1
Glass vials bottle	W	1
1000 μ l pipet	W	1
Petri dish	W	1
Hotplate magnetic stirrer	E	1
NEJE DK-8-KZ laser engraver	E	1
Temperature & Humidity Chamber	E	1
Digital multimeter	E	1

*Item category	
SP	Sample or specimen
C	Consumable
CH	Chemical
W	Labware, glassware, tool, and components
E	Equipment
S	Software

3.3 Methodology

3.3.1 Preparation of Coating Solution (Fire-Retardant and Lignin)

To enhance the thermal stability and conductivity of the paper substrate, a fire-retardant lignin-based coating solution was prepared as follows:

1. **Fire-retardant base solution:**

2.5 g of borax and 2.5 g of boric acid were dissolved in 100 mL of distilled water using a hotplate magnetic stirrer set to 80°C and 850 RPM (revolutions per minute), until a clear solution was obtained.

2. **Lignin dispersion:**

A portion of the prepared fire-retardant solution was transferred to fill half of a glass vial. Then, 0.8 g of lignin was gradually added and dissolved in the vial with gentle swirling.

3. **HEC addition:**

0.1 g of hydroxyethyl cellulose (HEC) was added to the remaining fire-retardant solution and stirred for 3 minutes to ensure complete dissolution.

4. **Final mixing:**

The lignin dispersion was slowly introduced into the HEC solution using a pipette and stirred for 10 minutes to ensure uniform mixing.

5. **Cooling:**

The final coating solution was allowed to cool to room temperature before use.

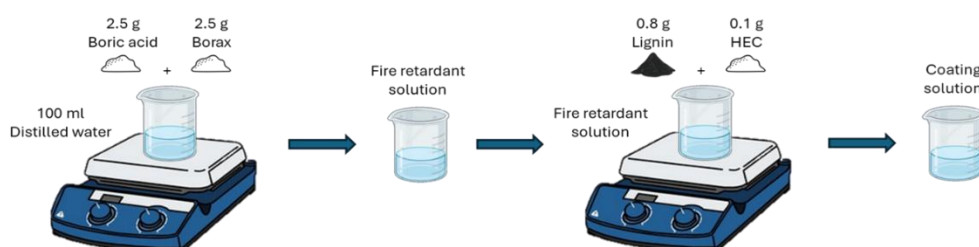


Figure 3.3.1: Preparation of coating solution.

3.3.2 Coating of Filter Paper

1. The cooled coating solution was poured into a Petri dish.
2. Sheets of filter paper were gently immersed in the solution for 15 minutes to ensure uniform coating and minimize bubble formation.

3. The coated papers were then removed and dried on a hotplate magnetic stirrer at a temperature of 50°C.
4. A clean, dry Petri dish was placed on top to apply gentle weight and ensure the paper remained flat during the drying process.

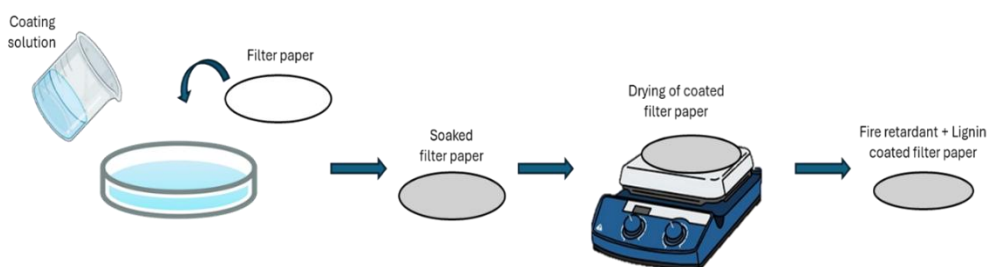


Figure 3.3.2: Coating filter paper.

3.3.3 Fabrication of MEG (using Laser-Induced Graphene)

1. The dried, coated filter papers were subjected to laser scribing using the NEJE DK-8-KZ laser engraver (405 nm wavelength) at a power output of 1.5 W and a scan speed of 17 mm/s.
2. The laser was initially applied while the paper was positioned flat (0° surface platform).
3. Laser scribing was then repeated with the paper tilted at angles of 5°, 10°, 15°, and 20°, simulating a gradual laser defocus from top to bottom.
4. This tilting strategy was designed to induce a concentration gradient in the laser-induced graphene, thereby enhancing the directional electron flow critical to MEG functionality.

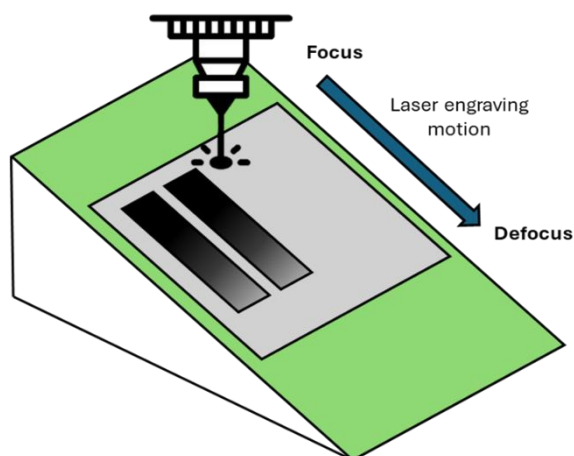


Figure 3.3.3: Schematic of MEG fabrication. Laser scribing with a gradual defocusing method.

Post-fabrication, the electrical conductivity of the samples was characterized using a four-point probe setup. Structural and compositional analyses were conducted via X-ray diffraction (XRD), scanning electron microscopy (SEM), and energy dispersive X-ray spectroscopy (EDX).

3.4 Performance Evaluation under Controlled Humidity Conditions

To evaluate the electrical performance of the fabricated paper-based MEG devices, voltage measurements were conducted under controlled humidity environments, with the setup as shown in Figure 3.4. The testing process was divided into two main phases: (i) performance comparison at a fixed humidity level across various paper tilting angles, and (ii) performance evaluation of the optimized sample under varying humidity conditions.

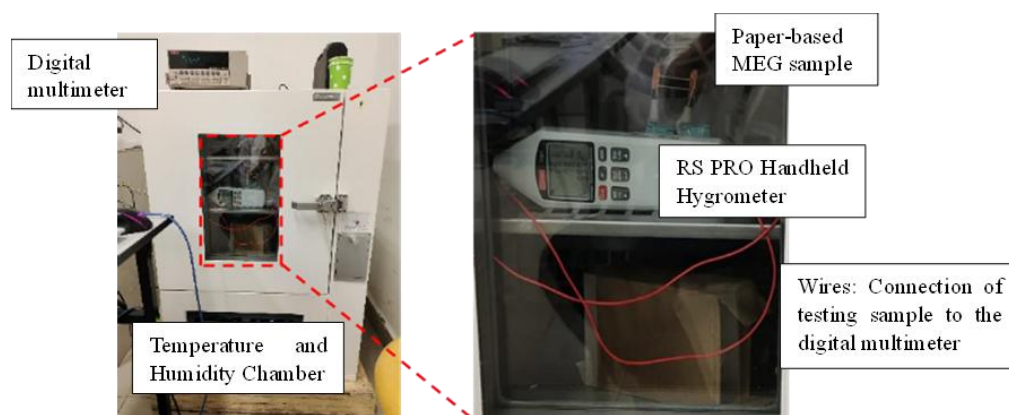


Figure 3.4: Voltage performance testing under set humidity conditions.

3.4.1 Voltage Measurement under Fixed Humidity

The initial phase aimed to assess the effect of the laser-induced gradient structure on voltage output. Five sets of MEG samples were fabricated using laser scribing, with paper angles of 0° , 5° , 10° , 15° , and 20° . These samples were individually placed inside a programmable temperature and humidity chamber, with relative humidity (RH) fixed at 80%.

- Each sample was allowed to stabilize inside the chamber before measurements were taken.
- Voltage output was recorded using a digital multimeter connected to the two ends of the laser-scribed region.

- This comparative evaluation enabled identification of the optimal scribing angle that yielded the highest voltage output and the most stable performance under constant humidity conditions.

3.4.2 Voltage Measurement under Varying Humidity

Following optimization, the sample exhibiting the best voltage and stability performance (as identified in Subsection 3.4.1) was selected for further testing under a range of relative humidity (RH) levels.

- The optimized MEG sample was subjected to controlled RH levels ranging from 40% to 90%, adjusted in 10% intervals within the humidity chamber.
- For each RH level, the sample was allowed to acclimate for a fixed period to ensure equilibrium before data collection.
- Voltage output was measured and recorded using a digital multimeter.
- All tests were conducted at room temperature, and each measurement was repeated at least three times to ensure consistency and reproducibility.

These performance evaluations under both fixed and variable humidity conditions provide critical insights into the moisture-induced electricity generation capability of the fabricated devices, as well as the influence of gradient structuring achieved through tilted laser scribing.

3.5 Summary

This chapter outlined the systematic approach used to fabricate and evaluate a self-powered flexible humidity sensor based on moisture-induced electricity generation (MEG). The methodology emphasized a low-cost, environmentally friendly strategy that utilizes lignin-coated filter paper as the substrate for generating laser-induced graphene (LIG) structures.

The chapter began with an introduction of the rationale behind the selected fabrication method, followed by a detailed list of all equipment,

chemicals, and materials used. The fabrication process was divided into three primary stages: preparation of the coating solution, coating of the filter paper, and fabrication of MEG structures via laser scribing. Fire-retardant additives (borax and boric acid) were incorporated into the lignin-based coating to enhance thermal stability and improve carbonization potential during laser exposure.

During MEG fabrication, laser scribing was performed first on flat surfaces and then at tilted angles (5° , 10° , 15° , and 20°) to create a gradient in laser focus. This gradient is hypothesized to induce variations in carbonization and conductivity, potentially enhancing the directional flow of charge carriers under humid conditions.

Finally, performance evaluation was conducted using a temperature and humidity chamber to measure the voltage response of each fabricated sample under fixed humidity levels. The optimized sample was selected for further testing across a broader humidity range (40% – 90% RH), with voltage output recorded using a digital multimeter.

Overall, the methodology presented in this chapter establishes a foundation for investigating the relationship between structural gradients, material composition, and humidity-induced electricity generation, which will be analyzed in detail in the following chapters.

CHAPTER 4

RESULTS AND DISCUSSION

4.1 Introduction

This chapter presents and discusses the experimental results obtained from the fabrication and performance evaluation of the self-powered flexible humidity sensor based on moisture-induced electricity generation (MEG). The primary objective is to analyze how variations in fabrication parameters – specifically the laser scribing angle – and environmental conditions, such as relative humidity, affect the electrical output of the device.

****Note:** All samples fabricated in this study have dimensions of 3 cm (*length*) x 1 cm (*width*).

4.2 Morphological and Structural Analysis

To verify the successful formation of laser-induced graphene (LIG) on the lignin-coated paper substrate, morphological and structural characterizations were performed using Scanning Electron Microscopy (SEM), Energy Dispersive X-ray Spectroscopy (EDX), and X-ray Diffraction (XRD). These analyses provide critical insights into the carbonization quality, surface morphology, and elemental composition of the laser-scribed regions.

4.2.1 SEM Analysis

SEM imaging was conducted on the surface of laser-scribed samples at a 15° tilt angle to observe the microstructure of the formed LIG. The SEM micrographs in Figure 4.2.1 revealed distinct morphological differences across the sample.

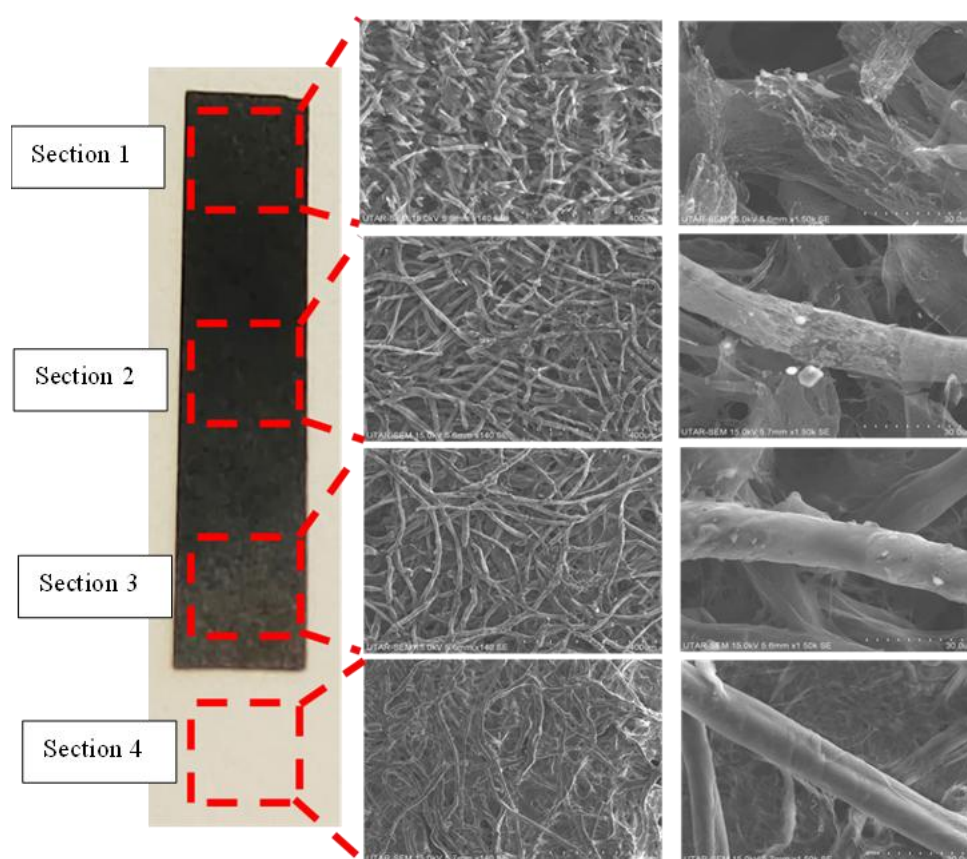


Figure 4.2.1: SEM test of the LIG sample.

In the bare paper section (Section 4), the surface exhibited a smooth texture with no visible porosity, indicating the presence of only the cellulose structure without evidence of laser-induced carbonization. In contrast, at a tilting angle of 15° , the surface became noticeably more porous and roughened, featuring randomly interconnected flake-like structures characteristic of well-formed LIG.

In this study, the LIG derived from lignin functions as both the active material and the electrode. Its 3D porous structure and surface morphology – which are tunable through laser scribing parameters – directly influence ion transport efficiency. This structural porosity offers two key benefits:

- **Enhanced moisture access:** The porous architecture increases surface area, facilitating greater penetration of water vapor into the material.

- **Increased interaction sites:** The internal pore walls contain functional groups that promote proton dissociation, contributing additional charge carriers to the system.

4.2.2 EDX Analysis

EDX analysis was performed to examine the elemental composition of the laser-scribed regions. The results in Figure 4.2.2 revealed a significant presence of carbon (C), confirming successful carbonization of the lignin-coated filter paper during laser irradiation. A notable presence of oxygen (O) was also detected, which is attributed to residual functional groups from lignin and cellulose, as well as possible surface oxidation.

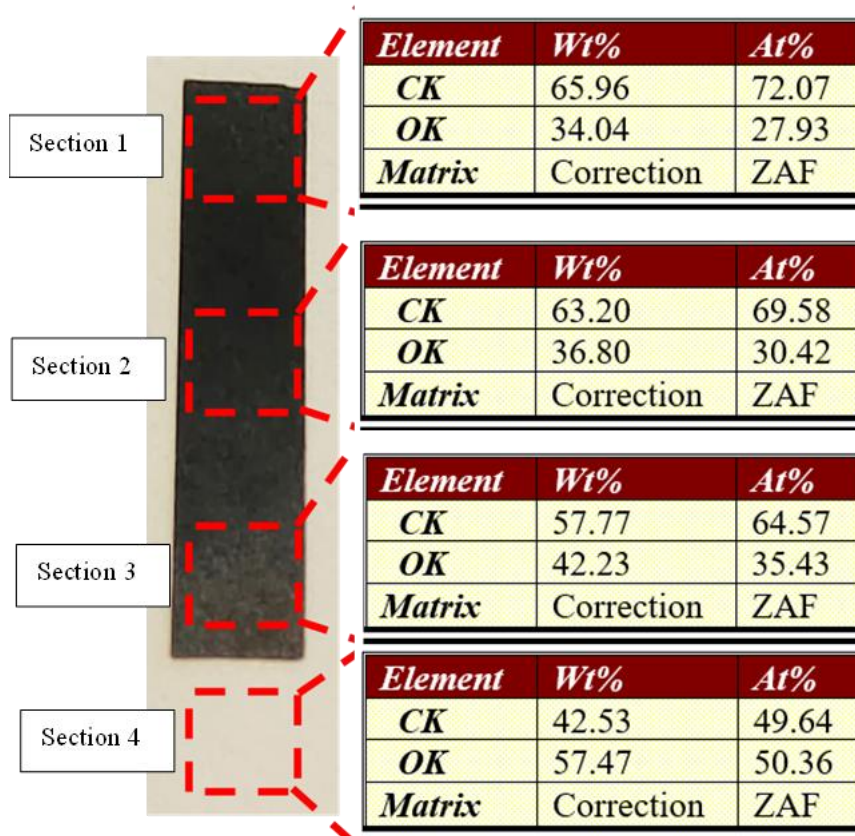


Figure 4.2.2: EDX spectrum of the LIG sample.

The carbon-to-oxygen ratios decreased by 8.19%, from 65.96 Wt% in Section 1 to 57.77 Wt% in Section 3, indicating reduced carbon content in Section 3 due to lower carbonization as the laser became progressively defocused.

4.2.3 XRD Analysis

XRD analysis was employed to examine the crystalline structure of the laser-scribe regions. According to the result in Figure 4.2.3, the sample exhibited a diffraction peak near $2\theta \approx 26.2^\circ$, corresponding to the (002) plane of graphitic carbon, which confirms the formation of layered graphene-like structures.

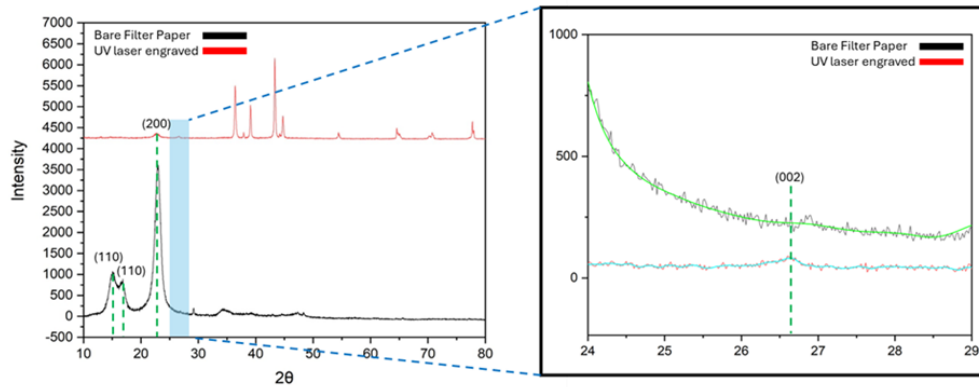


Figure 4.2.3: XRD spectrum of the LIG sample.

The presence of this crystalline (002) peak verifies the successful transformation of lignin into graphitic carbon, a critical factor for enhancing the electrical conductivity and overall performance of the MEG device.

4.3 Influence of Laser Tilting Angle on Voltage Output and Stability

Figure 4.3 (a) illustrates the average voltage output of MEG devices fabricated at paper tilting angles of 0° , 5° , 10° , 15° , and 20° , measured under fixed relative humidity (RH) of 80%. The results are presented as a bar graph to highlight variation across multiple experimental trials.

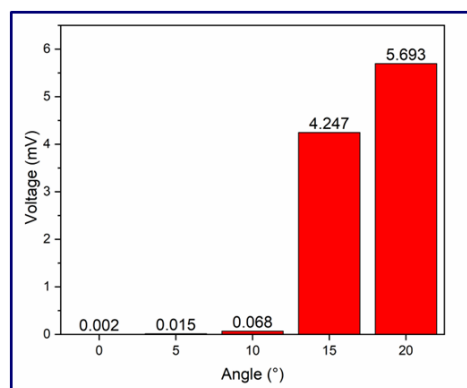


Figure 4.3 (a): Average voltage output of LIG samples at varying tilt angles under 80% RH.

The 20° tilt produced the highest average voltage output, reaching 5.693 mV, while the 0° and 5° samples generated significantly lower outputs at 0.002 mV and 0.015 mV, respectively. The data reveal a clear trend of increasing performance with greater tilt angle, supporting the hypothesis that tilting enhances the MEG effect through improved carbonization gradients and optimized surface morphology.

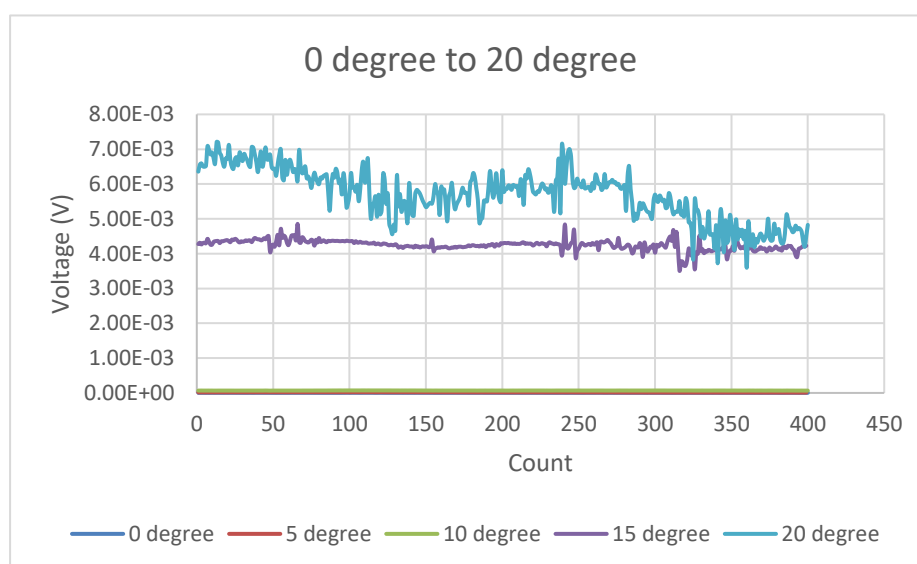


Figure 4.3 (b): Voltage output of LIG samples at varying tilt angles under 80% RH over time.

However, the result in Figure 4.3 (b) shows that signal for 20° sample exhibited considerable fluctuations, indicating poor stability. Stability is a critical parameter for sensor performance, as consistent and reliable output is essential for practical applications. In contrast, the sensor fabricated at a 15° tilt angle generated a slightly lower average output but exhibited significantly greater signal stability over time. Considering the trade-off between output performance and stability, the 15° sample was selected as the optimal configuration for further analysis.

4.3.1 Laser Defocus

Laser defocus refers to the deviation of the substrate surface from the laser's focal plane along the z-axis. When the paper is positioned at an incline during laser scribing, the laser beam interacts with the substrate at varying focal distances. As the laser moves from the elevated end of the tilted paper to the lower end, the degree of defocus gradually increases, creating a spatial energy gradient along the scribed path.

This defocus-induced variation affects two key laser parameters: spot diameter and fluence. A mild positive defocus increases the spot size while slightly reducing energy density, which promotes broader thermal diffusion. In contrast, excessive defocus results in insufficient fluence, preventing full carbonization. As a result, the graphitization efficiency varies along the scan direction, yielding a non-uniform LIG structure with potential for functional gradient formation.

The 15° tilt angle was found to offer optimal performance, likely due to its balances between energy input and thermal spread. At this angle, the laser transitions from near-focus to mild defocus, enabling both effective ablation and the formation of a carbonization gradient without excessive energy loss or incomplete conversion.

4.3.2 Concentration Gradient

One of the key mechanisms enabling voltage generation in the fabricated MEG device is the formation of a concentration gradient within the LIG structure, which interacts with ambient moisture to induce directional ion movement. This concept is analogous to findings in GO/rGO-based systems, where gradient distributions of oxygen-containing functional groups promote the diffusion of protons or other charge carriers under humid conditions.

Although the mechanism in LIG differs due to its more conductive, graphitic nature, the presence of a porous and chemically heterogeneous surface – enabled by gradient laser scribing – can still lead to local variations in surface potential and moisture absorption. This non-uniform distribution of

hydrophilic functional groups and surface resistance creates favorable conditions for localized charge separation and directed ion migration in humid environments, thereby enhancing voltage output.

The results of the tilt-angle optimization study highlight the importance of gradient engineering in the design of self-powered sensors. The ability to modulate LIG morphology and conductivity via simple geometric adjustments – such as varying the substrate tilt angle – offers a scalable and controllable strategy for improving device sensitivity and electrical performance. Future work may explore combining tilt-angle control with laser power modulation or post-treatment techniques to further refine functional gradients and tailor the device’s response characteristics.

4.4 Voltage Response of the Optimized Sample to Varying Humidity Levels

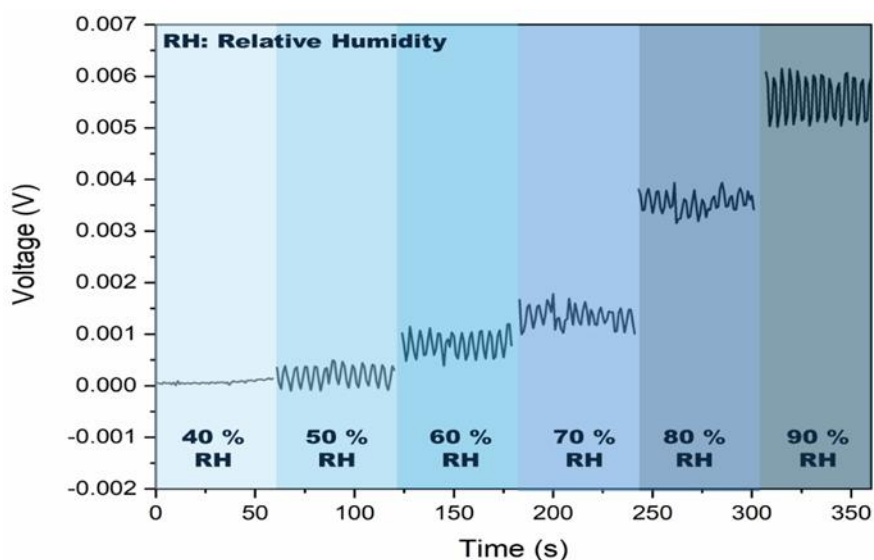


Figure 4.4: Voltage output under different relative humidity levels.

The experimental results demonstrate a clear and positive correlation between ambient humidity and the generated voltage. As shown in Figure 4.4, the voltage output increases progressively with rising RH, with a notably stronger response at higher humidity levels.

This trend suggests that moisture enhances the generation of charge carriers within the sensing material, thereby boosting the voltage output. The

relatively linear response between 40% and 90% RH indicates good sensitivity and consistent performance across this range.

4.4.1 Mechanism of Moisture-Induced Ion Transport

The MEG mechanism begins with the absorption of water from ambient air. Materials such as graphene oxide (GO), known for their high specific surface area and abundance of oxygen-containing functional groups (e.g., hydroxyl –OH and carboxyl –COOH), readily adsorb water molecules under humid conditions. Once absorbed, these water molecules promote proton dissociation, whereby the functional group release ionized hydrogen ions (H^+) into the material's structure.

In conventional GO-based MEG systems, a uniform structure is typically insufficient to generate an electric output. Instead, an asymmetric architecture or chemical gradient is necessary to establish a proton concentration difference. For instance, the research by Yang et al. (2018) states that in asymmetric porous graphene oxide membranes (a-GOMs), a region of partially reduced GO (P-rGO) is formed adjacent to pure GO. This engineered asymmetry induces spontaneous ion migration, with protons moving from areas of higher concentration (e.g., GO) toward areas of lower concentration (e.g., P-rGO).

This directed migration of protons leads to charge separation, resulting in a built-in electric potential across the material. When connected to an external circuit, this potential manifests as a measurable voltage output. The magnitude of this output is directly influenced by the density of mobile protons generated by moisture and the efficiency of their directional transport.

4.4.2 Sensor Response Characteristic and Humidity Sensitivity

The measured voltage response exhibits consistent and reproducible trends across repeated humidity cycles. The output increases proportionally from moderate to high relative humidity (RH) levels, highlighting the device's potential as a self-powered humidity sensor. However, the response curve may exhibit slight saturation due to:

- Complete hydration of available active sites
- A diminished proton concentration gradient as proton density becomes uniform
- Limited desorption at high RH levels, which affects dynamic ionic transport

Such saturation effects are commonly observed in GO-based sensors, where water uptake reaches equilibrium. Despite this, the relatively high voltage output maintained at 90% RH suggests strong sensitivity and effective surface interaction with moisture.

4.4.3 Influence of Environmental Factors

In this study, all experiments were conducted under controlled temperature conditions to isolate the effect of RH on sensor performance. However, in real-world applications, temperature and humidity interact and can jointly influence key factors such as ion mobility, proton dissociation, and diffusion rates. Therefore, future evaluations should consider the combined environmental effects to fully assess the sensor's performance under practical operating conditions.

4.5 Summary

This chapter presented a comprehensive analysis of the experimental findings related to the development and performance of a self-powered flexible humidity sensor based on laser-induced graphene (LIG) derived from lignin-coated paper. The study primarily investigated how variations in substrate tilt angle during fabrication, along with environmental humidity conditions, influence the morphological structure and voltage output of the sensor.

Morphological characterization using Scanning Electron Microscopy (SEM) confirmed the successful formation of porous graphene-like structures, with more pronounced 3D porosity observed at higher substrate tilt angles. This enhanced porosity is advantageous for moisture adsorption and ion transport. Energy Dispersive X-ray (EDX) analysis further verified a carbon-

rich composition, revealing a decreasing carbon-to-oxygen ratio at lower tilt angles, indicative of a gradient carbonization pattern. X-ray Diffraction (XRD) analysis also confirmed the presence of a (002) peak at approximately 26.2° , consistent with the formation of graphitic carbon structures within the LIG samples.

The voltage output of samples fabricated at tilt angles of 0° , 5° , 10° , 15° , and 20° was evaluated under fixed humidity conditions. Among these, the sample fabricated at a 15° tilt angle demonstrated a high voltage output of 4.247 mV and signal stability. This performance is attributed to the controlled laser defocus at that angle, which induces a functional gradient across the LIG layer, enhancing directional ion movement. This structural asymmetry promotes internal charge separation when exposed to moisture.

The optimized 15° sample was then tested under varying relative humidity levels (40% – 90% RH) to assess its sensing performance. Results showed a positive correlation between humidity and voltage output, confirming the sensor's capability for humidity-responsive energy harvesting. The underlying mechanism involves water molecule absorption by oxygen-containing functional groups within the graphene structure, leading to proton dissociation and the formation of an ion concentration gradient. This gradient drives hydrogen ion movement, resulting in charge separation and voltage generation. At higher humidity levels, response saturation may occur due to limited active sites and diffusion constraints.

Finally, the role of LIG surface characteristics – such as porosity and hydrophobicity – was discussed. The porous structure enhances the moisture interaction, while surface wettability affects water absorption and proton release. The study concludes that optimizing LIG morphology through precise control of laser parameters is critical for maximizing the performance of moisture-induced energy generation systems.

CHAPTER 5

CONCLUSIONS AND RECOMMENDATIONS

5.1 Conclusions

In this study, a self-powered flexible humidity sensor was successfully developed using laser-induced graphene (LIG) on a paper-based substrate. The research aimed to establish a cost-effective and environmentally friendly fabrication method for humidity sensors that operate without external power sources. The resulting device generated electricity through moisture-induced mechanisms and demonstrated promising performance in terms of voltage output across varying relative humidity (RH) levels.

The fabrication process involved direct laser engraving to form graphene structures on lignin-coated filter paper, yielding materials with good conductivity and hydrophilic characteristics – both essential for the hygroelectric effect. The sensor's voltage response showed a clear positive correlation with increasing humidity, confirming the viability of the MEG mechanism. Characterization techniques including XRD, SEM, EDX, and voltage measurements validated the formation of graphitic structures and the functional behavior of the device.

Overall, this project contributes to the advancement of eco-friendly, flexible, and self-sustaining sensors, with potential applications in wearable electronics, environmental monitoring, and health diagnostics.

5.2 Recommendations for future work

During the execution of this research, several challenges were encountered that provide insight into potential improvements for future studies:

1. Voltage Fluctuations and Signal Stability

Although a voltage response was observed, the signal sometimes fluctuated due to environmental noise and inconsistent moisture absorption. Surface treatment to enhance water adsorption-desorption balance could improve the sensor's stability.

2. Limited Durability and Reusability

The paper-based sensor showed limited mechanical robustness, especially under prolonged exposure to high humidity. Future studies can explore integrating biodegradable polymers or even clothes materials to enhance durability while maintaining eco-friendliness.

3. Quantitative Analysis of Moisture Generation Mechanisms

The current study focuses on qualitative relationships between RH and voltage output. Future work should include in-depth analysis of moisture-induced charge generation mechanisms, possibly via simulation models to optimize material properties and design.

REFERENCES

- Akinaga, H. (2020). Recent advances and future prospects in energy harvesting technologies. *Japanese Journal of Applied Physics*, 59(11), p.110201. doi: <https://doi.org/10.35848/1347-4065/abbfa0> (Akinaga, 2020)
- Ali, F., Raza, W., Li, X., Gul, H. and Kim, K.-H. (2019). Piezoelectric energy harvesters for biomedical applications. *Nano Energy*, 57, pp.879–902. doi: <https://doi.org/10.1016/j.nanoen.2019.01.012> (Ali et al., 2019)
- ANDIVI. (2020). *Humidity sensor what type should you choose?* [online] Available at: <https://www.andivi.com/humidity-sensor-what-type-should-you-choose/> (ANDIVI, 2020)
- Burcu Arman Kuzubasoglu (2022). Recent Studies on the Humidity Sensor: A Mini Review. 4(10), pp.4797–4807. doi: <https://doi.org/10.1021/acsaelm.2c00721> (Burcu Arman Kuzubasoglu, 2022)
- Chen, Z. and Lu, C. (2005). Humidity Sensors: A Review of Materials and Mechanisms. *Sensor Letters*, [online] 3(4), pp.274–295. doi: <https://doi.org/10.1166/sl.2005.045> (Chen and Lu, 2005)
- Cheng, H., Huang, Y., Zhao, F., Yang, C., Zhang, P., Jiang, L., Shi, G. and Qu, L. (2018). Spontaneous power source in ambient air of a well-directionally reduced graphene oxide bulk. *Energy & Environmental Science*, 11(10), pp.2839–2845. doi: <https://doi.org/10.1039/c8ee01502c>
- Delipinar, T., Shafique, A., Gohar, M.S. and Yapici, M.K. (2021). Fabrication and Materials Integration of Flexible Humidity Sensors for Emerging Applications. *ACS Omega*, 6(13), pp.8744–8753. doi: <https://doi.org/10.1021/acsomega.0c06106> (Delipinar et al., 2021)
- Edberg, J., Brooke, R., Hosseinaei, O., Fall, A., Wijeratne, K. and Sandberg, M. (2020). Laser-induced graphitization of a forest-based ink for use in flexible and printed electronics. *npj Flexible Electronics*, 4(1). doi: <https://doi.org/10.1038/s41528-020-0080-2>
- Ghomian, T. and Mehraeen, S. (2019). Survey of energy scavenging for wearable and implantable devices. *Energy*, 178, pp.33–49. doi: <https://doi.org/10.1016/j.energy.2019.04.088>
- Guo, J., Wen, R., Liu, Y., Zhang, K., Kou, J., Zhai, J. and Zhong Lin Wang (2018). Piezotronic Effect Enhanced Flexible Humidity Sensing of Monolayer MoS₂. *ACS Applied Materials & Interfaces*, 10(9), pp.8110–8116. doi: <https://doi.org/10.1021/acsaami.7b17529> (Guo et al., 2018)

- Gupta, B.D. and Ratnanjali (2001). A novel probe for a fiber optic humidity sensor. *Sensors and Actuators B-chemical*, 80(2), pp.132–135. doi: [https://doi.org/10.1016/s0925-4005\(01\)00899-1](https://doi.org/10.1016/s0925-4005(01)00899-1) (Gupta and Ratnanjali, 2001)
- Hong, S., Kim, J., Jung, S., Lee, J. and Shin, B.S. (2023). Surface Morphological Growth Characteristics of Laser-Induced Graphene with UV Pulsed Laser and Sensor Applications. *ACS Materials Letters*, 5(4), pp.1261–1270. doi: <https://doi.org/10.1021/acsmaterialslett.2c01222>
- Huang, Y., Cheng, H. and Qu, L. (2021). Emerging Materials for Water-Enabled Electricity Generation. *ACS Materials Letters*, 3(2), pp.193–209. doi: <https://doi.org/10.1021/acsmaterialslett.0c00474> (Huang, Cheng and Qu, 2021)
- Ilmira, N., Sheikh, S., Aziz, A., Salleh, N., Senawi, S., Hashim, A., Malik, A., Ali, M., Zu, M. and Yahya, A. (n.d.). *A Review on Classification, Types, and Properties of Humidity Sensors*. [online] Available at: <https://ir.uitm.edu.my/id/eprint/58488/1/58488.PDF> [Accessed 2 Mar. 2025]. (Ilmira et al., n.d.)
- Kharaz, A. and Jones, B.E. (1995). A distributed optical-fibre sensing system for multi-point humidity measurement. *Sensors and Actuators A: Physical*, 47(1-3), pp.491–493. doi: [https://doi.org/10.1016/0924-4247\(94\)00948-h](https://doi.org/10.1016/0924-4247(94)00948-h) (Kharaz and Jones, 1995)
- Kim, H.-S., Kang, J.-H., Hwang, J.-Y. and Ueon Sang Shin (2022). Wearable CNTs-based humidity sensors with high sensitivity and flexibility for real-time multiple respiratory monitoring. *Nano Convergence*, 9(1). doi: <https://doi.org/10.1186/s40580-022-00326-6> (Kim et al., 2022)
- Lee, C.-Y. and Lee, G.-B. (2003). Micromachine-based humidity sensors with integrated temperature sensors for signal drift compensation. *Journal of Micromechanics and Microengineering*, 13(5), pp.620–627. doi: <https://doi.org/10.1088/0960-1317/13/5/313> (Lee and Lee, 2003)
- Lee, C.-Y. and Lee, G.-B. (2005). Humidity Sensors: A Review. *Sensor Letters*, 3(1), pp.1–15. doi: <https://doi.org/10.1166/sl.2005.001> (Lee and Lee, 2005)
- Liang, Y., Ding, Q., Wang, H., Wu, Z., Li, J., Li, Z., Tao, K., Gui, X. and Wu, J. (2022). Humidity Sensing of Stretchable and Transparent Hydrogel Films for Wireless Respiration Monitoring. *Nano-Micro Letters*, 14(1). doi: <https://doi.org/10.1007/s40820-022-00934-1> (Liang et al., 2022)
- Lin, J., Peng, Z., Liu, Y., Ruiz-Zepeda, F., Ye, R., Samuel, E.L.G., Yacaman, M.J., Yakobson, B.I. and Tour, J.M. (2014). Laser-induced porous

- graphene films from commercial polymers. *Nature Communications*, [online] 5(1), p.5714. doi: <https://doi.org/10.1038/ncomms6714>
- Moon, H. and Ryu, B. (2024). Review of Laser-Induced Graphene (LIG) Produced on Eco-Friendly Substrates. *International Journal of Precision Engineering and Manufacturing-Green Technology*, 11(4), pp.1279–1294. doi: <https://doi.org/10.1007/s40684-024-00595-y>
- National Weather Service (2015). *Discussion on Humidity*. [online] Weather.gov. Available at: <https://www.weather.gov/lmk/humidity> (National Weather Service, 2015)
- Novoselov, K.S. (2004). Electric Field Effect in Atomically Thin Carbon Films. *Science*, 306(5696), pp.666–669. doi: <https://doi.org/10.1126/science.1102896>
- Pinheiro, T., Morais, M., Silvestre, S., Carlos, E., Coelho, J., Almeida, H.V., Barquinha, P., Fortunato, E. and Martins, R. (2024). Direct Laser Writing: From Materials Synthesis and Conversion to Electronic Device Processing. *Advanced materials (Weinheim. Print)*. doi: <https://doi.org/10.1002/adma.202402014>
- Pinheiro, T., Rosa, A., Ornelas, C., Coelho, J., Fortunato, E., Marques, A.C. and Martins, R. (2023). Influence of CO₂ laser beam modelling on electronic and electrochemical properties of paper-based laser-induced graphene for disposable pH electrochemical sensors. *Carbon Trends*, 11, pp.100271–100271. doi: <https://doi.org/10.1016/j.cartre.2023.100271>
- Raj, N., Nagamalleswara Rao Alluri, Venkateswaran Vivekananthan, Chandrasekhar, A., Khandelwal, G. and Kim, S.-J. (2018). Sustainable yarn type-piezoelectric energy harvester as an eco-friendly, cost-effective battery-free breath sensor. *Applied Energy*, 228, pp.1767–1776. doi: <https://doi.org/10.1016/j.apenergy.2018.07.016>
- Sensor Technology Handbook. (2005). Elsevier. doi: <https://doi.org/10.1016/b978-0-7506-7729-5.x5040-x> (Sensor Technology Handbook, 2005)
- Shen, D., Duley, W.W., Peng, P., Xiao, M., Feng, J., Liu, L., Zou, G. and Zhou, Y.N. (2020). Moisture-Enabled Electricity Generation: From Physics and Materials to Self-Powered Applications. *Advanced Materials*, 32(52), p.2003722. doi: <https://doi.org/10.1002/adma.202003722> (Shen et al., 2020)
- Sil, I., Mukherjee, S. and Biswas, K. (2017). A review of energy harvesting technology and its potential applications. *ENVIRONMENTAL AND EARTH SCIENCES RESEARCH JOURNAL*, 4(2), pp.33–38. doi: <https://doi.org/10.18280/eesrj.040202> (Sil, Mukherjee and Biswas, 2017)

- Sun, Z., Wen, X., Wang, L., Ji, D., Qin, X., Yu, J. and Ramakrishna, S. (2022). Emerging design principles, materials, and applications for moisture-enabled electric generation. *eScience*, [online] 2(1), pp.32–46. doi: <https://doi.org/10.1016/j.esci.2021.12.009> (Sun et al., 2022)
- Toh, W.Y., Tan, Y.K., Koh, W.S. and Siek, L. (2014). Autonomous Wearable Sensor Nodes With Flexible Energy Harvesting. *IEEE Sensors Journal*, 14(7), pp.2299–2306. doi: <https://doi.org/10.1109/jsen.2014.2309900>
- Wang, X., Deng, Y., Chen, X., Jiang, P., Cheung, Y.K. and Yu, H. (2021). An ultrafast-response and flexible humidity sensor for human respiration monitoring and noncontact safety warning. *Microsystems & Nanoengineering*, 7(1). doi: <https://doi.org/10.1038/s41378-021-00324-4> (Wang et al., 2021)
- Yang, C., Huang, Y., Cheng, H., Jiang, L. and Qu, L. (2018). Rollable, Stretchable, and Reconfigurable Graphene Hygroelectric Generators. *Advanced Science News*, 31(2), pp.1805705–1805705. doi: <https://doi.org/10.1002/adma.201805705>
- Ye, X., Yang, Z., Zheng, X., Qiang, H., Wei, M., Li, Y., Chen, M. and Luo, N. (2024). A review on the laser-induced synthesis of graphene and its applications in sensors. *Journal of Materials Science*. doi: <https://doi.org/10.1007/s10853-024-09883-z>
- You, S., Shi, H., Wu, J., Shan, L., Guo, S. and Dong, S. (2016). A flexible, wave-shaped P(VDF-TrFE)/metglas piezoelectric composite for wearable applications. *Journal of Applied Physics*, 120(23). doi: <https://doi.org/10.1063/1.4972478>
- Yu, Z. (2020). *Study of laser-induced graphene based flexible humidity sensor*. [online] Psu.edu. Available at: <https://etda.libraries.psu.edu/catalog/16463zqy5106> [Accessed 10 Mar. 2025]. (Yu, 2020)